Prestressing Concrete Structures with FRP Tendons

Reported by ACI Committee 440

*ACI encourages the development and appropriate use of new and emerging technologies through the publication of the **Emerging Technology Series**. This series presents information and recommendations based on available test data, technical reports, limited experience with field applications, and the opinions of committee members. The presented information and recommendations, and their basis, may be less fully developed and tested than those for more mature technologies. This report identifies areas in which information is believed to be less fully developed, and describes research needs. The professional using this document should understand the limitations of this document and exercise judgment as to the appropriate application of this emerging technology.*

Sami H. Rizkalla
Chair

John P. Busel
Secretary

Tarek Alkhrdaji	Edward R. Fyfe	Vistasp M. Karbhari	Morris Schupack
Charles E. Bakis	Ali Ganjehlou	James G. Korff	David W. Scott
P. N. Balaguru	Duane J. Gee	Michael W. Lee	Rajan Sen
Lawrence C. Bank	T. Russell Gentry	John Levar	Mohsen A. Shahawy
Abdeldjelil Belarbi	Janos Gergely	Ibrahim Mahfouz	Carol K. Shield
Brahim Benmokrane	William J. Gold	Henry N. Marsh	Khaled A. Soudki
Gregg J. Blaszak	Nabil F. Grace	Orange S. Marshall	Robert E. Steffen
Timothy E. Bradberry	Mark F. Green	Amir Mirmiran	Gamil Tadros
Gordon L. Brown	Mark Greenwood	Ayman S. Mosallam	Jay Thomas
Vicki L. Brown	Doug D. Gremel	Antonio Nanni	Houssam A. Toutanji
Thomas I. Campbell[*]	H. R. Hamilton	Kenneth Neale	Miroslav Vadovic
Charles W. Dolan[*]	Issam E. Harik	John P. Newhook	David Vanderpool
Dat Duthinh	Kent A. Harries	Max L. Porter	Milan Vatovec
Garth J. Fallis	Mark P. Henderson	Mark A. Postma	David White
Amir Fam	Bohdan Horeczko	Hayder A. Rasheed	

[*]Co-chairs of Subcommittee 440-I.
Note: The committee acknowledges the significant contribution of associate member Raafat El-Hacha.

Fiber-reinforced polymers (FRPs) have been proposed for use instead of steel prestressing tendons in concrete structures. The promise of FRP materials lies in their high-strength, lightweight, noncorrosive, nonconducting, and nonmagnetic properties. This document offers general information on the history and use of FRP for prestressing applications and a description of the material properties of FRP. The document focuses on the current state of design, development, and research needed to characterize and ensure the performance of FRP as prestressing reinforcement in concrete structures. The proposed guidelines are based on the knowledge gained from worldwide experimental research, analytical work, and field applications of FRPs used as prestressed reinforcement. The current development includes a basic understanding of flexure and axial prestressed members, FRP shear reinforcement, bond of FRP tendons, and unbonded or external FRP tendons for prestressing applications. The document concludes with a description of research needs.

CONTENTS

CHAPTER 1—INTRODUCTION

Fiber-reinforced polymer (FRP) composites have been proposed for use as prestressing tendons in concrete structures. The promise of FRP materials lies in their high-strength, lightweight, noncorrosive, nonconducting, and nonmagnetic properties. In addition, FRP manufacturing, using various cross-sectional shapes and material combinations, offers unique opportunities for the development of shapes and forms that would be difficult or impossible with conventional steel materials. Lighter-weight materials and preassembly of complex shapes can boost constructibility and efficiency of construction. At present, the higher cost of FRP materials suggests that FRP use will be confined to applications where the unique characteristics of the material are most appropriate. Efficiencies in construction and reduction in fabrication costs will expand their potential market. FRP reinforcement is available in the form of bars, grids, plates, and tendons. This document examines both internal and external prestressed reinforcement in the form of tendons.

One of the principal advantages of FRP tendons for prestressing is the ability to configure the reinforcement to meet specific performance and design objectives. FRP tendons may be configured as rods, bars, and strands as shown in Fig. 1.1. The surface texture of FRP tendons may vary, resulting in bond with the surrounding concrete that varies from one tendon configuration to another. Unlike conventional steel reinforcement, there are no standardized shapes, surface configurations, fiber orientation, constituent materials, and proportions for the final products. Similarly, there is no standardization of the methods of production, such as pultrusion, braiding, filament winding, or FRP preparation for a specific application. Thus, FRP materials require considerable engineering effort to use properly. Bakis (1993) has outlined manufacturing processes.

FRP tendons are typically made from one of three basic fibers. These fibers are aramid, carbon, and glass. Aramid fibers consist of a semicrystalline polymer known as aromatic polyamide. Carbon fibers are based on the layered graphene (hexagonal) networks present in graphite, while glass generally uses either E-glass or S-glass fibers. E-glass is a low-cost calcium-aluminoborosilicate glass used where strength, low conductivity, and acid resistance are important. S-glass is a magnesium-aluminosilicate glass that has higher strength, stiffness, and ultimate strain than E-glass. S-glass costs more than E-glass, and both are susceptible to degradation in alkaline environments. Table 1.1 gives properties of typical fibers.

The selection of the fiber is primarily based on consideration of cost, strength, stiffness, and long-term stability. Within these fiber groups, different performance and material

Table 1.1—Typical fiber properties

	High-modulus carbon (Thornel 2004)	Intermediate-modulus carbon (Torayca 1996)	Standard-modulus carbon (Torayca 1996)	Aramid (Kevlar 1992)	E-glass (Hartman, Greenwood, and Miller 1994)	S-glass
Tensile strength, GPa	2.1 to 2.4	5.4 to 6.3	3.5 to 4.9	2.9 to 3.0	3.4	4.9
Tensile modulus, GPa	517 to 827	294	230	71 to 112	72.3	86.9
Ultimate strain, %	0.3	1.9 to 2.2	1.5 to 2.1	2.4 to 3.6	4.8	5.7
Mass density, g/cm^3	2.0 to 2.2	1.8	1.8	1.44	2.58	2.46
Diameter, μm	10	5	7	12	3 to 24	6 to 14
Longitudinal CTE, ppm/°C	–1.5	–0.6	–0.4	–4 to –5	5.4	1.6

Note: 1 GPa = 145 ksi; 1 g/cm^3 = 62.4 lb/ft^3; 1/°C = 1.8/°F; 1 μm = 4×10^{-5} in.; CTE = coefficient of thermal expansion.

characteristics may be achieved. For example, aramids may come in low, high, and very high modulus configurations. Carbon fibers are also available with moduli ranging from below that of steel to several multiples of that of steel. Of the several fiber types, glass-based FRP reinforcement is least expensive and generally uses either E-glass or S-glass fibers.

The resins used for fiber impregnation are usually thermosetting and may be polyester, vinylester, epoxy, phenolic, or polyurethane. The formulation, grade, and physical-chemical characteristics of resins are practically limitless. The possible combinations of fibers, resins, additives, and fillers make generalization of the properties of FRP tendons very difficult. Additionally, FRP composites are heterogeneous and anisotropic. Final characteristics of an FRP tendon are dependent on fiber and resin properties, as well as the manufacturing process. Specific details of a particular tendon should be obtained from the manufacturer of the tendon.

1.1—Organization and limitations of document

The emphasis of this document is on flexural members in concrete buildings and bridges pretensioned with aramid or carbon FRP tendons. An FRP prestressing system consists of the tendon and the anchorage. Properties, performance, and overall behavior are dependent on the tendon/anchorage system and on the individual components. Performance of independent elements should be verified by test. Information is provided for bonded and unbonded post-tensioned applications where it is available. Only fully prestressed members are considered, with no attempt being made to address partially prestressed members. In general, to account for the brittle characteristics of FRP, unlike steel, which is ductile, the recommendations herein are conservative. Specific limitations of FRP tendons are addressed and research needs are listed in Chapter 9. The committee feels that this document is relevant to simple spans and to spans made continuous by placing steel reinforcement in the deck of a bridge structure. No recommendations are made for beams made continuous with FRP tendons or for moment-resisting frames where ductility or large deformations are required for seismic loading. The worldwide number of prestressed FRP applications is less than 100 (MDA 2004; IABSE 2003). Most are bridge structures where issues of fire were not considered critical.

Fig. 1.1—Sample FRP reinforcement configurations.

1.2—Historical development and use of FRP reinforcement

The concept of using short glass fiber reinforcement in concrete was first introduced in the 1930s but was not developed into long fiber reinforcement for nearly two decades. In the 1950s and 1960s, the U.S. Army Corps of Engineers was sufficiently interested in long glass fibers for reinforcement that a series of comprehensive reports was compiled (Mather and Tye 1955; Pepper and Mather 1959; Wines, Dietz, and Hawley 1966). Although these reports were generated, research and site applications were limited. In the 1970s, corrosion-induced deterioration of concrete structures, particularly bridge decks, led to a renewed interest in design strategies that would reduce susceptibility of structures to corrosive environments.

In the 1970s, research activities started in Germany on glass FRP-based prestressing tendons. In 1978, a joint venture between German contractor Strabag-Bau and German chemical producer Bayer resulted in glass fiber-reinforced polymer (GFRP) tendons and an anchorage system for post-tensioning applications. These tendons were incorporated in several bridges in Germany and Austria. After various transition stages, however, Strabag stopped its activities in this field in the early 1990s. The National Bureau of Standards (NBS)—now renamed the National Institute of Standards and Technology (NIST)—examined nonmetallic rods for antenna guy wires. In the process, they conducted some of the first research into anchorage of composite rods that became relevant to prestressed concrete application of FRP materials (NBS 1976).

Interest in the corrosion-resistant properties of nonmetallic bars and tendons continued to grow in the 1980s. In 1983, AKZO, a chemical producer in the Netherlands, and HBG, a contractor, jointly developed aramid fiber reinforced polymer (AFRP) prestressing tendons. The Japanese have also undertaken an extensive national program to examine the use of FRP reinforcement in concrete structures. Around 1980, research and development began in Japan on production techniques for FRP reinforcement and its application to concrete structures. This research and development originally focused on the development of FRP-reinforced concrete members that used FRPs instead of steel reinforcing bars and prestressing tendons. In the United States, a new anchorage was developed for glass fiber tendons (Iyer and Kumarswamy 1988), and the prestressing use of Kevlar™ was investigated (Dolan 1989). Iyer's anchorage was supported financially by the Florida Department of Transportation (FDOT), which funded a major study to investigate the prestressing application of glass fiber tendons for bridge and marine substructures (Sen, Issa, and Mariscal 1992). This research culminated in the first conference to focus on FRP composites for civil engineering applications (Iyer and Sen 1991), and the construction of the first FRP prestressed bridge in Rapid City, South Dakota (Iyer 1993). These and similar efforts led to the development of several commercial tendon systems, many of which are discussed in the proceedings of the First International Symposium for FRP in Reinforced Concrete Structures (FRPRCS-1) (Nanni and Dolan 1993), and in a Japanese Society of Civil Engineers publication (JSCE 1996).

1.3—Design guidelines and technical committees

In 1993, the first design guidelines for FRP-reinforced and prestressed concrete buildings were established by the Japanese Society of Civil Engineers. The Japanese version of the guideline was released in 1995, while the English version (Sonobe et al. 1997) was published in 1997. The Canadian Standards Association has produced two standards—CAN/CSA S6-00 and CAN/CSA S806-02—that contain code provisions for the use of FRP prestressing tendons in bridges and buildings, respectively.

In Europe, unified design guidelines for FRP reinforcement are under development. A task group with this aim was established at the end of 1996, within the former CEB (Euro-International Concrete Committee). In December 1997, a 4-year training and mobility of researchers network project, titled "Development of Guidelines for the Design of Concrete Structures, Reinforced, Prestressed or Strengthened with Advanced Composites," started. This so-called "ConFiber-Crete Network" was comprised of 11 teams from nine different European countries.

Since the merger of CEB and FIP (*Federation Internationale de la Precontrainte*), this task group has been integrated in the new *fib* (*Federation Internationale du Béton*). Task Group 9.3 of *fib* Commission 9 is charged with developing design guidelines for concrete structures reinforced, prestressed, or strengthened with FRP, based on the design format of the CEB-FIP Model Code and Eurocode 2 (*fib*

TG9.3). Recent activities in Europe have been summarized by Matthys and Taerwe (2001).

The American Society of Civil Engineers (ASCE) established a standards committee to address stand-alone FRP products. The Transportation Research Board (TRB) has formally established Committee A2C07 to examine the use of FRP in bridge structures. Other societies, including the Society for the Advancement of Material and Process Engineering (SAMPE) and the Market Development Alliance (MDA) of the FRP Composites Industry, have been active in the area of FRP for construction use.

1.4—Research efforts

Early development work on prestressing with FRP was carried out at the South Dakota School of Mines by Iyer who developed the first prestressing anchorage in the late 1980s. The first glass fiber prestressed bridge built in the United States was in Rapid City, South Dakota, in 1990. Other research was carried out at the University of South Florida, Florida Atlantic University, and the Florida Department of Transportation (Sen, Issa, and Mariscal 1992). Studies included static and fatigue testing of beams and half-scale bridges, durability studies, and full-scale testing of piles. All three materials—aramid, carbon, and glass—were evaluated.

Work relating to FRP prestressing in the United States has been documented by Dolan (1999). Much of the research on FRP reinforcement in the United States has been conducted by individual investigators at the University of Arizona (Eshani, Saadatmanesh and Nelson 1997), the University of Michigan (Naaman and Jeong 1995), the Massachusetts Institute of Technology (Triantafillou and Deskovic 1991), Pennsylvania State University (Nanni et al. 1996a,b), South Dakota School of Mines (Iyer et al. 1996), the University of California (Long Beach), West Virginia University (Vijay and GangaRao 2001), the University of Wyoming (Dolan et al. 2000), and Lawrence Technological University (Grace 2000a,b). In 1993, FHWA sponsored research into accelerated aging and standardized testing of FRP materials at Georgia Institute of Technology, Pennsylvania State University, and the Catholic University of America. In 1994, FHWA sponsored research into development of design recommendations for FRP prestressing for bridge girders that led to design specification recommendations for AASHTO (Dolan et al. 2000). Lawrence Technological University has developed a demonstration bridge using external unbonded FRP tendons (Grace 1999).

In Canada, several researchers, mostly within ISIS Canada (Canadian Network of Centers of Excellence on Intelligent Sensing for Innovative Structures), have been investigating applications of FRP prestressing tendons. Work at the University of Manitoba has emphasized carbon FRP tendons and has considered the behavior of prestressed beams under both service and ultimate conditions (Abdelrahman, Tadros, and Rizkalla 1995; Fam, Rizkalla, and Tadros 1997). Extensive studies on bond and transfer length have also been conducted. At the Royal Military College of Canada (RMC), work has been done on aramid FRP tendons (McKay and Erki 1993), and more recently on carbon FRP tendons. Researchers at Queen's University have been investigating

the low temperature and long-term behavior of beams prestressed with CFRP (Bryan and Green 1996). Additionally, the possibility of using CFRP rods to prestress bridge deck slabs was investigated (Braimah, Green, and Soudki 1996), and work on the transfer length of beams prestressed with carbon FRP was conducted (Soudki, Green, and Clapp 1997). Partially prestressed, partially bonded FRP tendons have been investigated (Rizkalla, Fang, and Campbell 2001). Noncorrosive wedge-type anchorages for FRP tendons have been developed at the University of Calgary (Sayed-Ahmed and Shrive 1998; Campbell et al. 2000; Shaheen 2004). At the University of Sherbrooke, extensive investigations are being conducted into the durability of FRP rods for reinforcing and prestressing concrete, and into the development of a bond-type anchorage (Zhang 2002). The effects of temperature on beams prestressed with FRP tendons have been the focus of research at Concordia University, and applications of unbonded FRP tendons have been considered at the University of Windsor (Salib, Abdel-Sayed, and Grace 1999). Researchers at Carleton University and the University of Waterloo are also investigating applications of FRP prestressing tendons.

The decline in the Japanese economy in the 1990s slowed the Japanese development program and has curtailed the availability of many Japanese products for evaluation and testing in North America. Developments in Japan have been addressed by Fukuyama (1999), and details of some recent projects are available from the Advanced Composites Cables (ACC) Club.

Activities in Europe relating to the use of FRP have been reported by Taerwe and Matthys (1999). Of the projects financially supported by the European community, the BRITE/EURAM project, "Fiber Composite Elements and Techniques as Non-Metallic Reinforcement for Concrete," started November 1991 and ended in 1996. The Universities of Braunschweig and Ghent, together with industrial partners from Germany and The Netherlands, investigated performance characteristics and structural aspects of FRP reinforcement for prestressed and reinforced concrete members. The EUROCRETE project, a pan-European collaborative research program with partners from the United Kingdom, the Netherlands, Switzerland, France, and Norway, began in December 1993 and ended in 1997. This project included material development, research on durability in aggressive environments, determination of structural behavior, and development of design guidance, techno-economic, and feasibility studies. The project included construction of demonstration structures.

1.5—Demonstrations and field applications

During the late 1980s and throughout the 1990s, several demonstration projects have shown the potential of FRP prestressing applications. The Marienfelde Bridge in Berlin, completed in 1988, is the first structure to be built in Germany since 1945 with external unbonded prestressing (Wolff and Miesseler 1989). It is a two-span, 27.61 m (90.5 ft) and 22.98 m (75.1 ft) continuous double-T section beam providing a pedestrian walkway and a bridle path. Seven external Polystal® tendons, each composed of 19 glass fiber

Fig. 1.2—Construction of the FRP prestressed girders for the Taylor Bridge in Headingly, Manitoba, Canada.

bars, are located between the beam webs. Each tendon has a working load of 600 kN (135 kip), is 7.5 mm (0.3 in.) in diameter, and is covered with a 5 mm (0.2 in.) thick sheathing. Four bars out of a group of 19 in a tendon slipped out of the anchorage during prestressing. The treatment for bar slippage was not very difficult because the external prestressing system readily permitted replacement of the entire tendon, complete with the duct and anchorages, at both ends.

The BASF bridge in Ludwigshafen, Germany, is a prestressed roadbridge (Zoch et al. 1991). The bridge girder has width for two lanes, and the total length is 85 m (278 ft). Four CFRP tendons were used in conjunction with 16 conventional steel tendons as internal unbonded post-tensioned reinforcement. Each tendon consisted of 19 carbon fiber-reinforced polymer (CFRP) strands of 12.5 mm (0.5 in) diameter, with a prestressing force of 70 kN (16 kip) applied on each strand. The die-cast/wedge anchorage was chosen for applying prestress by post-tensioning to the bridge girder. All tendons were guided through tubes embedded in the concrete, steel tendon tubes were filled with cement grout after tensioning, while the CFRP tendon tubes were not filled to allow inspection, exchange of tendons, and data collection.

In 1993, a bridge was built in Calgary using FRP pretensioned tendons incorporating fiber optic sensors (Rizkalla and Tadros 1994). This was the first bridge of its kind in Canada and one of the first in the world. A second bridge incorporating FRP prestressing tendons was built at Headingly, Manitoba, in 1997. Figure 1.2 shows the fabrication of the prestressed girders for the Taylor Bridge in Headingly, and Fig. 1.3 shows the completed bridge.

Figures 1.4 and 1.5 show the Bridge Street Bridge in Southfield, Michigan. This bridge was completed in 2001 and is a three-span structure that used bonded and unbonded CFRP tendons in both longitudinal and transverse directions (Grace et al. 2002). The Bridge Street Bridge Deployment Project consists of two parallel, independent bridges (Structure A and Structure B) over the Rouge River in the City of Southfield, Michigan. Both structures are designed to accommodate one traffic lane and incorporate three 15-degree skewed spans. Structure A consists of new substructure and superstructure and incorporates five

Fig. 1.3—Completed Taylor Bridge in Headingly, Manitoba, Canada.

Fig. 1.5—Completed Bridge Street Bridge (Grace et al. 2002).

Fig. 1.4—Erection of the Bridge Street Bridge, Southfield, Mich. (Courtesy of HRC Consulting Engineers, Inc., Mich.)

equally spaced conventional AASHTO-I beams in each of the three spans, with a continuous cast-in-place concrete deck slab. Structure B consists of twelve double T (DT) beams, each prestressed using pretensioned Leadline tendons and post-tensioned, in the longitudinal and transverse directions, using carbon fiber composite cable (CFCC) strands. Details of the construction of the Bridge Street Bridge can be found elsewhere (Grace, Enomoto, and Yagi 2002). Bridge Structures A and B were designed for two traffic lanes using the provisions to the extent possible of the American Association of State Highway and Transportation Officials (AASHTO) Standard

Specifications for Highway Bridges (sample calculations in Grace and Singh [2003]). The superstructure dead loads for Structure B included the DT beams, composite CFRP-reinforced concrete topping, surfacing mixture, pedestrian sidewalk, barrier wall, and the bridge parapet and railing. Live load design was based on the Michigan MS-23 standard truck loading. This live load condition corresponds to 125% of the Michigan MS-18 (AASHTO HS20-44) standard truck loading. The live load distribution factor used for design of the DT beams was calculated two different ways, using provisions defined in both the AASHTO Standard and AASHTO LRFD Bridge Design Specifications.

Four demonstration projects, in which FRP pretensioned concrete piles have been driven successfully, have been carried out in the United States. Further details of these projects are given in Chapter 8.

1.6—Definitions
Definitions of terms used in concrete structures are found in "Cement and Concrete Terminology (ACI 116R)." Terms and notation that have specific application to FRP reinforcement and prestressing are defined as follows.

A
AFRP—aramid fiber-reinforced polymer.

alkalinity—the condition of having or containing hydroxyl (OH$^-$) ions; containing alkaline substances. Note: in concrete, the alkaline environment has a pH above 12.

anchor—in prestressed concrete, to lock the stressed tendon in position so that it will retain its stressed condition.

anchorage—In post-tensioning, a device used to anchor the tendon to the concrete member; in pretensioning, a device used to maintain the elongation of a tendon during the time interval between stressing and release.

anchorage, dead-end—the anchorage at that end of a tendon that is opposite to the jacking end.

B
balanced FRP reinforcement ratio—the reinforcement ratio in a flexural member that causes the ultimate strain of FRP and the ultimate compressive strain of concrete to be simultaneously attained.

bar—a nonprestressed FRP element, made mostly of continuous fibers with nominally rectangular or circular cross section, used to reinforce a structural concrete component; the bar may have a deformed or roughened surface to enhance bonding with concrete.

bond stress—the stress between the concrete and the reinforcing element.

bond stress, average—the force in a reinforcing element divided by the product of the perimeter and the development length of the reinforcing element.

bond, transfer—in pretensioning, the bond stress resulting from the transfer of stress from the tendon to the concrete.

bonded member—a prestressed concrete member in which the tendons are bonded to the concrete either directly or through grouting.

bonded tendon—prestressing tendon that is bonded to concrete either directly or through grouting.

C

camber—a deflection that is intentionally built into a structural element or form to improve appearance or to nullify the deflection of the element under the effects of loads, shrinkage, and creep.

CFRP—carbon fiber-reinforced polymer.

coefficient of thermal expansion—change in linear dimension per unit length.

composite—a combination of one or more materials differing in form or composition on a macroscale. Note: the constituents retain their identities; that is, they do not dissolve or merge completely into one another, although they act in concert. Normally, the components can be physically identified and exhibit an interface between one another.

concrete clear cover—the least distance from the concrete surface to the nearest surface of embedded prestressing tendon or reinforcement.

creep—the inelastic strain of a material under a sustained load over a period of time.

creep-rupture—the tensile fracture of a material subjected to sustained high stress levels over a period of time.

D

deformability—ratio of deflection parameter of a member at ultimate to the same parameter at cracking.

development length—length of embedded reinforcement required to develop the nominal capacity of a member.

duct—a conduit for post-tensioning tendons.

E

effective depth of section—distance measured from the extreme compression fiber to the centroid of the tensile reinforcement.

effective prestress—stress remaining in prestressing tendons after all losses have occurred.

embedment length—length of embedded reinforcement provided beyond a critical section.

F

fiber, aramid—highly oriented organic fiber derived from polyamide incorporating an aromatic ring structure.

fiber, carbon—fiber produced by the heating and stretching for molecular alignment of organic precursor materials containing a substantial amount of carbon, such as rayon, polyacrylonitrile (PAN), or pitch, in an inert environment.

fiber content—the amount of fiber present in a composite. Note: this usually is expressed as a percentage volume fraction or weight fraction of the composite.

fiber-reinforced polymer (FRP)—composite material consisting of continuous fibers impregnated with a fiber-binding polymer, then molded and hardened in the intended shape.

fiber volume fraction—the ratio of the volume of the fibers to the total volume of the fiber-reinforced composite.

H

harped tendons—tendons that have a trajectory that is bent with respect to the center of gravity axis of the concrete member.

J

jacking force—the temporary force exerted by the device that introduces tension into prestressing tendons.

L

limit states—those conditions of a structure in which it ceases to fulfill the relevant function for which it was designed.

load factor—factor applied to a specified load that, for the limit state under consideration, takes into account the variability of the loads and load patterns, and analysis of their effects.

load, factored—product of a specified load and its load factor.

load, sustained—specified dead load plus that portion of the specified live load expected to act over a period of time sufficient to cause significant long-term deflection.

loss, elastic—in prestressed concrete, the reduction in prestressing load resulting from the elastic shortening of the member.

loss, friction—the stress loss in a prestressing tendon resulting from friction between the tendon and duct or other device during stressing.

loss, shrinkage—reduction of stress in prestressing tendon resulting from shrinkage of concrete.

loss of prestress—the reduction in the prestressing force that results from the combined effects of slip at anchorage, relaxation of stress, frictional loss, and the effects of elastic shortening, creep, and shrinkage of the concrete.

M

matrix—the material that serves to bind the fibers together, transfer loads to the fibers, and protect them against environmental attack and damage due to handling.

P

post-tensioning—a method of prestressing in which the tendons are tensioned after the concrete has hardened.

prestressed concrete—concrete in which the internal stresses have been initially introduced so that the subsequent stresses resulting from dead load and superimposed loads are counteracted to a desired degree; this may be accomplished by post-tensioning or pretensioning.

pretensioning—a method of prestressing in which the tendons are tensioned before the concrete is placed.

pultrusion—a continuous process for manufacturing composites that have a uniform cross-sectional shape; the process consists of pulling a fiber-reinforced material through a resin impregnation bath then through a shaping die where the resin is subsequently cured.

R

relaxation—the loss of tension with time in a stressed tendon maintained at constant length and temperature.

resistance factor—factor applied to a specified material property or to the resistance of a member for the limit state under consideration, which takes into account the variability of dimensions, material properties, workmanship, type of failure, and uncertainty in the prediction of resistance.

S

splitting tensile strength—tensile strength of concrete determined by a concrete cylinder splitting test.

strand—a linear component that constitutes either a part or the whole of a prestressing tendon.

T

tendon—an element such as a wire, bar, rope, a single strand, or an assembly of multiple strands used to impart prestress to a structural component. Note: Distinction is made between strands and tendons. Strands refer, for example, to pultruded FRP rods and tendons to bundled FRP rods stressed by common anchors.

thermoplastic—resin that is not cross-linked, and generally can be remelted and recycled.

thermoset—resin that is formed by cross-linking polymer chains and cannot be melted or recycled because the polymer chains form a three-dimensional network.

tow—an untwisted bundle of continuous fibers.

transfer—act of transferring force in prestressing tendons from jacks or the pretensioned anchorage to the concrete member.

transfer length—the length from the end of the member where the tendon stress is zero, to the point along the tendon where the prestress is fully effective, also called transmission length.

V

vinyl esters—a class of thermosetting resins containing esters of acrylic, methacrylic acids, or both, many of which have been made from epoxy resin.

1.7—Notation

A_p = cross-sectional area of FRP tendon, mm^2 (in.^{2})

A_{pi} = cross-sectional area of FRP tendon at level i, mm^2 (in.^{2})

$A_{p\ int}$ = area of the internal prestressed reinforcement, mm^2 (in.^{2})

$A_{p\ tot}$ = total area of internal and external prestressed reinforcement, mm^2 (in.^{2})

A_s = area of nonprestressed tensile reinforcement, mm^2 (in.^{2})

A_s' = area of nonprestressed compressive reinforcement, mm^2 (in.^{2})

A_v = amount of FRP shear reinforcement within spacing s, mm^2 (in.^{2})

$A_{v,min}$ = minimum amount of FRP shear reinforcement within spacing s, mm^2 (in.^{2})

a = depth of the equivalent compression block, mm (in.)

b = width of compression face of member, mm (in.)

b_w = width of web (width of a rectangular cross section), mm (in.)

c = depth of neutral axis, mm (in.)

c_u = depth of neutral axis at ultimate, mm (in.)

DI = deformability index

d = depth to the FRP tendon (distance from extreme compression fiber to centroid of tension reinforcement), mm (in.)

d_b = diameter of reinforcing bar, mm (in.)

d_e = effective depth, mm (in.)

d_i = depth to the FRP tendon in layer i, mm (in.)

d_p = depth from the concrete top fiber to the centroid of the prestressing tendon, mm (in.)

d_{pu} = depth of the external prestressing tendons at ultimate limit state, mm (in.)

E_c = modulus of elasticity of concrete, MPa (psi)

E_f = modulus of elasticity of the fibers, MPa (psi)

E_p = modulus of elasticity of the prestressed tendon, MPa (psi)

E_r = elastic modulus of the resin, MPa (psi)

e_{eff} = effective eccentricity, mm (in.)

f = maximum stress in tendon due to combined axial load and harping, MPa (psi)

f_c = concrete stress in the extreme compression fiber, MPa (psi)

f_c' = specified compressive strength of concrete, MPa (psi)

f_{ci}' = compressive strength of concrete at time of initial prestress, MPa (psi)

f_{fb} = stress in the bent FRP stirrup, MPa (psi)

f_{fu} = ultimate tensile strength of the FRP stirrup, MPa (psi)

f_h = stress in tendon induced by harping, MPa (psi)

f_i = FRP stress in tendon layer i, MPa (psi)

f_m = stress increase in bottom layer of FRP tendons due to flexure, MPa (psi)

f_p = tendon stress, MPa (psi)

f_{pe} = effective stress in tendon (after allowance for all prestress losses), MPa (psi)

f_{pu} = design ultimate tensile strength of prestressed FRP tendon and anchorage system, MPa (psi)

f_y = yield strength of nonprestressed tensile reinforcement, MPa (psi)

f_y' = yield strength of nonprestressed compressive reinforcement, MPa (psi)

h_f = depth of the flange in T-section, mm (in.)

I_{cr} = cracked moment of inertia, mm^4 ($in.^4$)

I_e = effective moment of inertia, mm^4 ($in.^4$)

I_g = gross moment of inertia, mm^4 ($in.^4$)

k = ratio of neutral axis depth to FRP tendon depth

k_b = bond correction factor

k_u = ratio of neutral axis depth to FRP tendon depth for an over-reinforced section

L = effective span of beam, length of the prestressing tendon between anchorages, mm (in.)

L_d = development length, mm (in.)

L_{fb} = flexural bond development length, mm (in.)

L_t = transfer length, mm (in.)

l_{tfh} = tail length of the FRP stirrup, mm (in.)

M = unfactored live load moment, N-mm (in.-lb)

M_a = maximum moment in a member at which the deflection is being computed, N-mm (in.-lb)

M_{cr} = cracking moment, N-mm (in.-lb)

M_n = nominal moment capacity, N-mm (in.-lb)

m = number of layers of tendons

n = modular ratio = E_f/E_c

n_r = modular ratio of the resin = E_r/E_f

P_j = jacking load, N (lbf)

R = radius of curvature of the harping saddle (radius of saddle), mm (in.)

r = radius of the bend of the FRP stirrup or radius of FRP tendon, mm (in.)

REL = relaxation losses, %

R_d = depth reduction factor, %

R_f = relaxation component due to relaxation of the fibers, %

R_p = relaxation component due to the relaxation of the polymer matrix

R_s = relaxation component due to straightening of the fibers

R_t = radius of the tendon, mm (in.)

S_d = spacing of the deviators, mm

s = stirrup spacing or pitch of continuous spirals, mm (in.)

y_{cr} = distance from the extreme compression fiber to the neutral axis of the cracked section, mm (in.)

y_{eff} = distance from the extreme compression fiber to the effective neutral axis, mm (in.)

V_c = shear resistance provided by concrete, N (lbf)

V_{frp} = shear resistance provided by FRP stirrups, N (lbf)

V_n = nominal shear strength of a reinforced concrete cross section, N (lbf)

V_p = vertical component of prestressing force, N (lbf)

V_s = shear resistance provided by steel stirrups, N (lbf)

V_u = factored shear load, N (lbf)

v_f = volume of fibers in the tendon

v_r = volume of resin in the tendon

α = factor used in Eq. (3-24)

α_{fb} = factor for the flexural bond length of FRP tendon

α_t = factor for the transfer length of FRP tendon

β_1 = stress-block factor for concrete

β_b = factor for softening equivalent moment of inertia

Δf_p = change in stress in an unbonded prestressed tendon due to flexure, MPa (psi)

$\Delta\varepsilon_p$ = change in strain in prestressed tendon due to flexure

ε_{cp} = average strain in concrete at centroid of the tendon

ε_{cu} = ultimate strain in concrete in compression

ε_d = additional strain in tendon that causes the extreme precompressed fiber to reach zero strain (decompression)

ε_f = strain available in tendon for flexure after decompression

ε_p = tendon strain

ε_{pe} = effective strain in the FRP tendon after all losses

ε_{pi} = initial elastic strain in FRP tendon

ε_{pr} = loss of strain capacity due to sustained loads

ε_{ps} = strain in the FRP tendon at service

ε_{pu} = ultimate tensile strain in the prestressed FRP tendons

ϕ = strength reduction factor

ϕ_{bend} = strength reduction for bent stirrup

λ = material constant

ρ = reinforcement ratio

ρ_b = balanced reinforcement ratio

ρ_i = reinforcement ratio for reinforcement at level i

Ω = strain reduction coefficient

Ω_u = strain reduction coefficient at ultimate

ξ = ratio of effective stress to ultimate tensile strength

ψ_i = ratio of depth of tendon layer i to depth of bottom tendon layer

CHAPTER 2—FRP TENDONS AND ANCHORAGES

2.1—FRP tendon characterization

FRP tendons are produced from a wide variety of fibers, resins, shapes, and sizes. Only aramid and carbon fibers, however, are recommended in this document. Glass fibers have poor resistance to creep under sustained loads and are more susceptible to alkaline degradation than carbon and aramid fibers. An FRP tendon is identified by the type of fiber used to make the tendon. The Japanese have developed a system to define FRP tendons (Table 2.1).

The tendon and anchorage comprise a system. The tendon properties are developed for a specific anchorage. Using an alternative anchorage may not result in the same strength and performance properties of the system.

2.2—Commercial tendons

Properties and characteristics of commercially available tendons are summarized in Table 2.2 and are based on the manufacturer's published data. The trade names of the products

are used for clarity and historical perspective. Not all tendons are currently available, and the properties of the tendons are subject to change. Some of these tendons are shown in Fig. 1.1.

2.3—Description of tendons

Arapree®—Arapree® was a combined development of AKZO Chemicals and Hollandsche Beton Groep in The Netherlands. The manufacturing rights have been transferred to Sireg S.P.A., an Italian company. Arapree® consists of aramid (Twaron®) fibers embedded in epoxy resin. Two types of cross section are available in the marketplace: rectangular and circular. The former is easier to grip with a wedge-type anchorage (Gerritse and Werner 1988).

The anchorage developed for Arapree®, both flat and round rod types, consists of a tapered metal sleeve into which the tendon is either grouted (post-tensioning application) or clamped between two wedges. The wedge anchorage, designed primarily for temporary use, is comprised of a steel sleeve and two semicylindrical tapered wedges made of

Polyamide PA6. The outer surface of the wedges and the inner surface of the metal socket are smooth and noncoated. The inner surface of the wedge, which holds the tendon, is similarly smooth, and gripping of the tendon relies solely on the frictional resistance provided by the plastic.

FiBRA—Mitsui Construction Company of Japan produces an FRP rod known as FiBRA. Braiding of fiber tows, followed by epoxy resin impregnation and curing, form the rod. Aramid and carbon fibers have been used, with aramid being the most common. Small variations in the manufacturing process produce two types of rod: rigid and flexible. Rigid rods are used for concrete reinforcement, whereas flexible rods, which can be coiled, are used as prestressing tendons (Tamura, Kanda, and Tsuji 1993).

FiBRA has two different types of anchorage: a resin-potted anchorage used for single-tendon anchoring and a wedge anchorage for either single- or multiple-tendon anchoring. This wedge anchorage is made of four steel wedges (held together by an O-ring) that slip inside a steel sleeve with a conical interior surface. Grit is applied to the inner surface of the wedges. The exterior surface of the wedges and the interior surface of the steel sleeve are coated with a dry lubricant to assist in seating and removal of the anchorage.

Technora®—Technora® tendon is an aramid product jointly developed by Sumitomo Construction Company and Teijin Corporation, both of Japan. Technora® is a spirally wound pultruded tendon impregnated with a vinyl ester resin (Noritake et al. 1993). Manufacturing of a spirally wound tendon begins with pultruding the impregnated straight fiber

Table 2.1—Fiber identification

Fiber type	Identification
Aramid fiber	A
Carbon fiber	C
Multiple fibers	*

[*]In a tendon using multiple fibers, the first letter of the two fibers making up the material will be used with the dominant fiber going first (for example, CA for carbon/aramid composite with carbon having the larger volume).

Table 2.2—Properties of FRP tendons (compiled from various references)

Property	AFRP				CFRP	
	Arapree®	FiBRA	Technora®	Parafil®	Leadline™	CFCC
Fiber	Twaron	Kevlar49	Technora	Kevlar49	Carbon	Carbon
Resin	Epoxy	Epoxy	Vinyl ester	—	Epoxy	Epoxy
Fiber volume ratio	0.45	0.65	0.65	—	0.65	0.65
Density, g/cm^3	1.25	1.28	1.3	1.44	1.53	1.5
Longitudinal tensile strength, GPa	1.2 to 1.5	1.25 to 1.4	1.7 to 2.1	1.2 to 1.9	2.25 to 2.55	1.8 to 2.1
Transverse tensile strength, MPa	—	30	—	—	57	—
Longitudinal modulus, GPa	62 to 64	65 to 70	54	120 to 130	142 to 150	137
Transverse modulus, GPa	—	5.5	—	—	10.3	—
In-plane shear strength, MPa	—	4.9	—	—	71	—
In-plane shear modulus, GPa	—	2.2	—	—	7.2	—
Major Poisson's ratio	0.38	0.34 to 0.6[*]	0.35	—	0.27	—
Minor Poisson's ratio	—	0.02	—	—	0.02	—
Bond strength, MPa	7.7	10 to 13	10 to 16	—	4 to 20	7 to 11
Maximum longitudinal strain, %	2.4	2.0 to 3.7	3.7 to 3.8	1.5 to 1.7	1.3 to 1.5	1.57
Maximum transverse strain, %	—	—	—	—	0.6	—
Longitudinal compressive strength, MPa	—	335	—	—	1440	—
Transverse compressive strength, MPa	—	158	—	—	228	—
Longitudinal thermal expansion coefficient/°C	-2×10^{-6}	-2×10^{-6}	-3×10^{-6}	—	-0.9×10^{-6}	0.5×10^{-6}
Transverse thermal expansion coefficient/°C	50×10^{-6}	60×10^{-6}	—	—	27×10^{-6}	21×10^{-6}
Relaxation ratio at room temperature, % loss from jacking stress	11 to 14	12 at 103 h	8 to 13 at 103 h	6 to 9 at 105 h	2 to 3	0.5 to 1 at 102 h

[*]Pseudo Poisson's ratio due to structure of tendon.

Notes: A "—" indicates that information is not available or is not applicable. 1 MPa = 145 psi; 1 GPa = 145 ksi; 1 g/cm^3 = 62.4 lb/ft^3; and 1/°C = 1.8/°F.
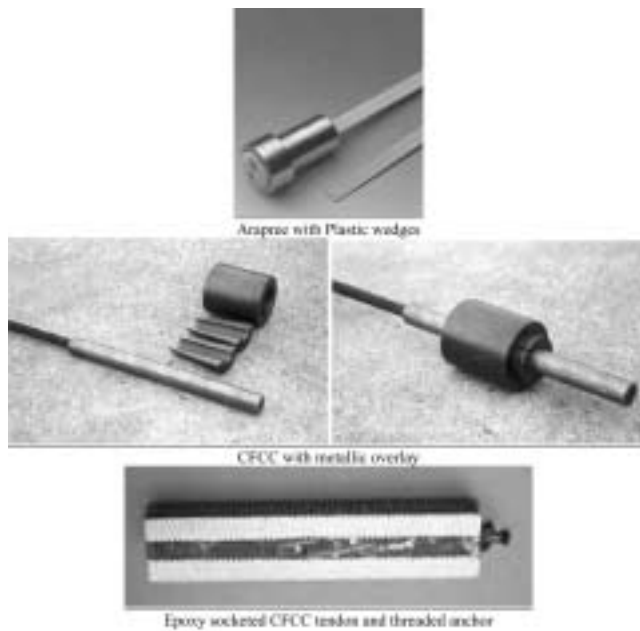
Fig. 2.1—Photos of representative anchorages.

bundles through an unheated die. Identical fiber bundles are spirally wound around the tendon to produce a deformed surface. Longitudinal fiber bundles are added to the outer surface before a second spiral winding is added. The product is then cured in an oven.

Technora® tendons employ either wedge-type or potted-type anchorages. Anchorages for single rod tendons or multiple rod tendons, numbering from three to 19 rods, are available. A screw thread is cut into the outer surface of the housing so that the anchorage can be secured with a nut onto a bearing plate.

Parafil®—Linear Composites Limited of England is the producer of a parallel-lay tendon composed of dry fibers contained within a protective polymeric sheath (Burgoyne 1988). Parafil® was originally developed in the early 1960s to moor navigation platforms in the North Atlantic. Parafil® has several features that distinguish it from other FRP prestressing tendons: it cannot be bonded to concrete; it contains no resin; and it was not initially developed for prestressing. Nevertheless, it has been used for prestressing concrete on a number of occasions.

Parafil® tendons are anchored by means of a barrel and spike fitting, which grips the fibers between a central tapered spike and an external matching barrel. Aluminum alloy, galvanized mild steel, stainless steel, and composite materials may be used for the anchorages because this scheme takes advantage of the fibers of the tendon simply being tightly packed in the protective outer sheathing.

Leadline™— Mitsubishi Kasei Corporation of Japan has developed a CFRP tendon called Leadline™ that is pultruded and epoxy impregnated. There are several varieties of Leadline™ tendons that differ in pattern and method of fabrication of their surfaces. Smooth tendons have no surface deformations. Indented tendons have two shallow helical depressions in the surface that spiral in opposite

directions. Ribbed tendons have either raised helical windings similar to the indented pattern or a circumferential winding transverse to the longitudinal axis of the tendon.

Leadline™ employs a steel wedge system to anchor the tendons with an aluminum sleeve that fits between the wedges and the tendon. The sleeve has four independent arms that extend along the length of the tendon. The wedges are placed around the sleeve so that the gap between adjacent wedges falls over the solid portion of the sleeve. The sleeve is intended to spread the stresses imposed on the tendon by the wedges. A plastic film is placed around the whole assembly to secure the multiple pieces together for insertion into the steel sleeve.

CFCC—Carbon fiber composite cable (CFCC) was developed by Tokyo Rope Mfg. Co., Ltd. and Toho Rayon Co., both of Japan. The tendon is formed by twisting a number of rods in a manner similar to a conventional stranded steel tendon (Santoh 1993). Materials used for CFCC include PAN-based carbon fiber and epoxy resin developed by Tokyo Rope. Multiple pieces of prepreg (semi-hardened tows with a resin precursor) are made into a bundle that is treated with a proprietary coating and formed into a small-diameter rod. A number of these rods are stranded and formed into a composite tendon that is heated and cured to form the finished product. The coating protects the tendon from UV radiation and mechanical damage while increasing the bond characteristics with concrete.

The manufacturer classifies CFCC anchoring methods as resin-filling and die-cast methods. The anchorages are chosen based on the intended application. The resin-filling method bonds the tendon to a steel cylinder utilizing a high-performance epoxy. These cylinders can be threaded as necessary to allow anchoring with nuts. The die-cast method attaches a die-molded alloy and steel tube to the tendon. Steel wedges then clamp the steel tube in a similar manner to steel tendon systems. Several commercial tendon/anchorage systems have been tested and evaluated by Nanni et al. (1996a,b). Some of these anchorages are shown in Fig. 2.1.

2.4—Anchorage characterization

The various types of anchorages used with FRP tendons can be classified as clamp, plug and cone, resin sleeve, resin potted, metal overlay, and split wedge anchorages, and are shown in Fig. 2.2. These anchorages are briefly described as follows.

2.4.1 *Clamp anchorage*—A clamp anchorage consists of grooved steel plates sandwiching the FRP rod and held together by bolts. The force is transferred from the tendon to the anchorage by a shear-friction mechanism and is influenced by parameters such as the roughness of the interface surfaces and the clamping force applied by the bolts. The performance of the anchorage is improved by using a sleeve material (protection media) to encase the tendon. This intermediary material with low stiffness and high ultimate elongation smooths the lateral pressure distribution on the tendon (Malvar and Bish 1995). The length of the anchorage may be varied, depending on the material chosen to ensure that the ultimate strength of the tendon is reached.
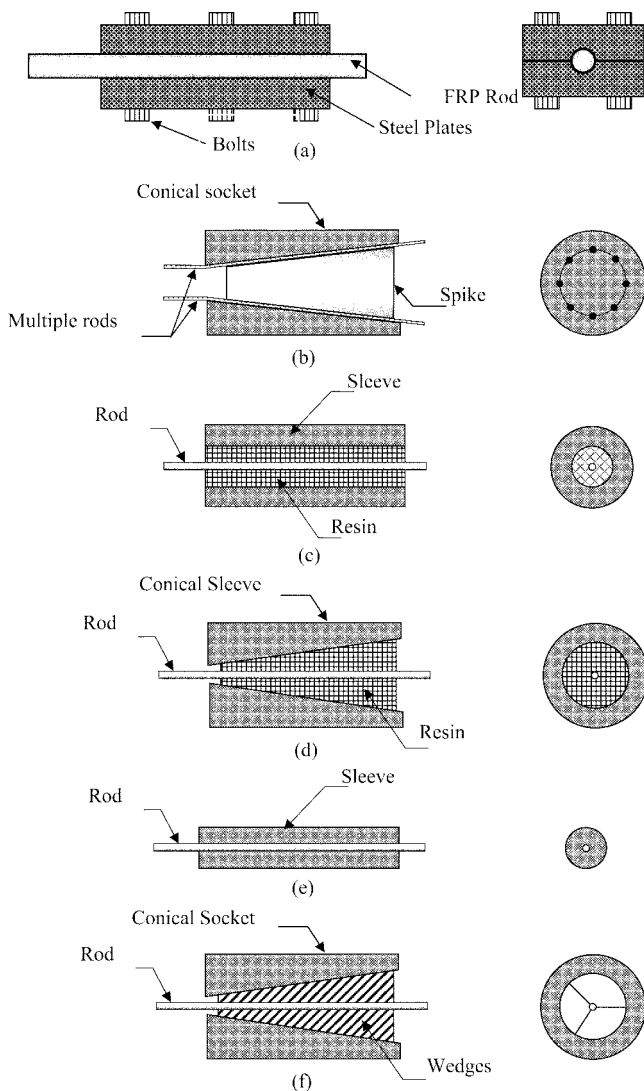
Fig. 2.2—(a) Clamp; (b) plug and cone; (c) straight sleeve; (d) contoured sleeve; (e) metal overlay; and (f) split wedge anchorages.

2.4.2 *Plug and cone anchorage*—The plug and cone (or barrel and spike) anchorage is made of a socket housing and a conical spike (Burgoyne 1988). Such a system is particularly well suited to anchor Parafil® tendons where the aramid fibers are not encased in resin media, but are held only by an outer protective sheath. Parafil® is unique in its ability to evenly distribute the aramid fibers around the spike, thereby achieving high anchorage efficiency. The gripping mechanism of the anchorage is similar to that of a wedge anchorage, where the tendon is held by the compressive force applied to the fiber by inserting the spike into the barrel. This compressive stress, together with the friction between the rod material and the socket, in addition to the spike, generate a frictional stress that resists the slipping of the tendon out of the socket. The field application of this system requires the removal of the plastic sheath, combing and spreading of the individual fibers, and proper placement of the spike with a uniform distribution of fibers all around it.

2.4.3 *Straight sleeve anchorage*—In this anchorage, the FRP tendon is embedded in resin that fills a tubular metallic

housing such as steel or copper. The potting material ranges from nonshrink, cement, with or without sand, to expansive cement to epoxy-based materials. In the case of nonshrink cement and polymeric potting materials, the load-transfer mechanism depends completely on bonding and interlocking between the anchorage components. The mechanism of load transfer is by bond at the interface between the rod and the filling material, and between the filling material and the metallic sleeve. To increase the bond between the anchorage components in such cases, an internally threaded sleeve is used, or a rigid filler material, such as sand, is added to the resin, or both. Filler in the resin also serves to reduce chemical shrinkage of the resin during curing. To enhance the bond between the tendon and the grout material, surface modifications such as braiding, twisting, or ribs can be applied to the tendon.

Harada and coworkers were among the earliest users of expansive cementitious materials to fill straight metallic sleeve anchorages (Harada et al. 1993). Expansive cement generates significant lateral pressure and increases the slipping resistance of the tendon. The 25 to 40 MPa (3600 to 5800 psi) internal radial pressures developed by the expansive cementitious materials are adequate for gripping FRP tendons with a wide range of surface configurations without causing undue stress concentrations at the point of egress of the tendon during quasistatic and cyclic loadings (Harada et al. 1997). Anchorages as long as 300 to 400 mm (12 to 16 in.) have been shown to be sufficient for developing the full strength of CFRP tendons without slippage at the free end of the anchorage. The effectiveness of such anchorages has also been demonstrated in elevated temperature, extended duration relaxation tests (Dye, Bakis, and Nanni 1998). At this time, the main shortcoming of this type of anchorage appears to be the 2- to 3-day curing time for expansive cementitious materials.

2.4.4 *Contoured sleeve anchorage*—The contoured sleeve anchorage has the same components as the straight sleeve anchorage. The principal difference between the two systems is the varied profile of the inner surface of the contoured sleeve, which may be linearly tapered or parabolically tapered. The load-transfer mechanism from the tendon to the sleeve is by interface shear stress, which is a function of bonding, and radial stress produced by the variation of the potting material profile. A conical profile with a constant taper angle is the most popular type of resin potted anchorage. Kim and Meier (1991) developed a variable stiffness anchorage for CFRP tendons. The work was based on concepts of a commercial anchorage developed by the Swiss company BBR. The anchorage was made of a cone filled with an epoxy matrix containing high-modulus ceramic filler. Holte, Dolan, and Schmidt (1993) described a parabolic anchorage with epoxy/sand filler.

The following parameters affect the performance of a resin potted anchorage: length of the anchorage, angle of the anchorage cone, front radius of anchorage cone, modulus of elasticity of the potted material, and length and modulus characteristic of the "soft zone" in resin filler at the front of the anchorage. Potted anchorages often fail through pullout of the tendon from the resin/grout rather than by rupture of

the tendon. Practical drawbacks with this anchor include precutting the tendons to length and the curing time for the potting material.

2.4.5 *Metal overlaying*—The die-cast wedge system for CFCC requires that the tendon length be predefined so that a metal tube can be cast onto the tendon at a specific location during fabrication with the result that adjustment on site is limited. The metal overlay is added to the ends of the tendon by means of die-molding during the manufacturing process. The die-cast molding can then be gripped at the location of the metal material using a typical wedge anchorage. The use of this system is limited because of the inflexibility in the specified length of the tendon. The load transfer in this anchorage is achieved by shear (friction) stress, which is a function of the radial compressive stress and the friction at contact surfaces.

2.4.6 *Split-wedge anchorage*—Split-wedge anchorages are generally preferred because of their compactness, ease of assembly, reusability, and reliability. This type of anchorage can be subdivided into two categories: systems with direct contact between plastic or steel wedges and the tendon, and systems using a sleeve between the wedges and the tendon. Wedge anchorages are widely used in anchoring steel tendons but should be modified for use with FRP tendons by increasing their length to reduce transverse stress on the tendon and controlling roughness in the wedge to prevent notching the tendon. The number of the wedges in the split-wedge anchorage varies from two to six wedges inserted into the barrel. The main reason for increasing the number of wedges is to provide a smoother lateral stress distribution in the radial direction of the tendon. The mechanism of gripping relies on friction and clamping force between the wedges, barrel, and tendon. Using a small taper on the wedges is of great importance to provide a smooth and uniformly distributed transverse stress.

A metallic anchorage was developed as part of the ISIS Canada program (Sayed-Ahmed and Shrive 1998; Campbell et al. 2000) for 8 mm Leadline™ CFRP tendons. The anchorage consists of three components: a stainless steel barrel with a conical socket; a four-piece stainless steel conical wedge set and a thin, soft metal sleeve that is placed between the wedges and the tendon. The distinct feature of the anchorage is that the taper angle of the wedge is 0.1 degrees greater than that of the inner surface of the barrel. The difference in angle between the barrel and the wedges helps to produce more desirable radial stress distribution on the tendon and ensures that failure of the tendon occurs outside the anchorage. An experimental and analytical investigation of this anchorage has been reported by Al-Mayah, Soudki, and Plumtree (2001). Nonmetallic versions of this anchorage, in which the elements are made either from ultra-high-performance concrete (UHPC), where the barrel is wrapped with CFRP sheet, or from carbon fiber reinforced reactive powder concrete, have been developed and tested by Reda Taha and Shrive (2003a,b) and Shaheen (2004), respectively.

2.4.7 *Failure modes of anchorages*—Various failure modes have been observed with wedge anchorages and FRP tendons,

and these are summarized by separating them into two main categories: failure of the anchorage system, and rupture.

*   **Failure of the anchorage system**—This kind of failure can be classified into four modes:

    1. *Movement or slip of the tendon out of the anchorage caused by insufficient grip (low shear force) between the tendon and sleeve*—Grip can be increased by increasing the friction at the contact surfaces, by increasing the normal force applied, or both.

    2. *Slip of the sleeve and tendon together relative to the wedges*—This indicates a high shear force between the tendon and sleeve together with a lower shear force between the sleeve and wedges. This can be overcome in the same manner as mentioned in 1.

    3. *Slip of the wedges relative to barrel*—This rarely happens, mainly because of the design and geometrical configuration of the wedges and the barrel. It is often accompanied by crushing of the tendon.

    4. *Rupture of the rod inside the anchorage*—High stress concentrations can be generated in the tendon inside the anchorage, causing damage of the fibers. An anchorage design that results in low stress concentration and uniform load distribution in the anchor overcomes this problem.

*   **Failure of the tendon outside the anchorage**—If the tendon does not break in or within three diameters of the anchorage, then the anchorage is not contributing to the failure of the tendon and is considered a satisfactory anchorage design.

CHAPTER 3—FLEXURAL DESIGN
3.1—General considerations

Numerous flexural tests on FRP prestressed members are reported in the literature. Comprehensive testing began in the mid 1980s in Japan on beams with carbon and aramid tendons, and in Europe on beams with aramid and glass tendons (Gerritse and Werner 1991). The first tests in the United States were conducted on beams with aramid tendons (Dolan 1990). In the intervening years, several attempts have been made to combine these data into design or performance recommendations (FIP 1992; JSCE 1992). The lack of uniform testing protocols and consistent reporting procedures made completion of these criteria very difficult.

A conventional prestressed concrete beam with steel tendons will deform elastically until cracking, and then the rate of member deflection will progressively increase as the tendons yield until failure occurs by concrete crushing or tendon rupture. On the other hand, an FRP prestressed beam will deform elastically until cracking, then continue to deform in an approximate linear manner under increasing load until the tendon ruptures or the ultimate concrete compression strain is exceeded. These two behaviors are compared in Fig 3.1. The lower modulus of elasticity of FRP (Table 2.2) is reflected in the lower post-cracking behavior.

Flexural design limit states include service level stresses and flexural strength requirements. Service level stresses may be computed using techniques similar to those for conventional prestressed concrete. The loss of prestress in FRP tendons is caused by the following factors:
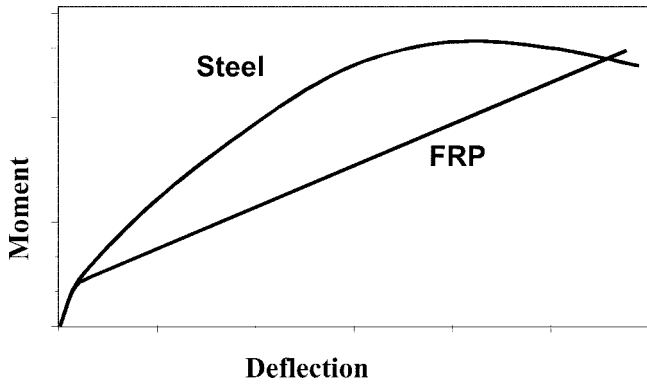
Fig. 3.1—Schematic representation of moment-deflection responses of prestressed concrete elements.

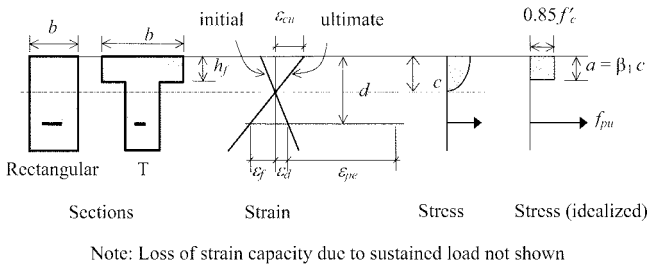Note: Loss of strain capacity due to sustained load not shown

Fig. 3.2—Balanced ratio: stress and strain conditions.

- Anchorage seating at transfer of prestress;
- Creep of the concrete;
- Shrinkage of the concrete;
- Elastic shortening of the concrete; and
- Relaxation of the tendons.

Anchorage seating loss is a function of the tendon system. Losses due to creep, shrinkage, and elastic shortening of concrete may be calculated using standard methods for concrete sections prestressed with steel tendons (PCI 1975, 2000); however, the modulus of elasticity of the FRP tendon should be used in place of the modulus of elasticity of steel. Losses for FRP tendons due to these three sources are typically less than the corresponding losses for steel tendons due to the lower modulus of elasticity of FRP tendons. Relaxation losses are more problematic and are less well understood, as there is little experimental data available that describes relaxation loss profiles for FRP tendons. Relaxation characteristics vary with the fiber type (Table 2.2) and are projected to be less than 12% of the initial level of prestress over the life of the structure (ACI 440R; JSCE 1993). More details are given in Section 3.10.

3.2—Strength design methodology

The approach to strength design of FRP prestressed beams is based on the concept of a balanced ratio, which is defined as the reinforcement ratio that simultaneously results in rupture of the tendons and crushing of the concrete. Concrete failure is taken as an extreme compression strain of ε_{cu} = 0.003. This strain limit assumes no allowance is made for confinement of concrete due to the presence of closed stirrups. A rectangular stress block is used to model the concrete behavior. Tendon failure is defined as occurring when the strain in the tendon reaches the ultimate tensile strain capacity ε_{pu}.

3.3—Balanced ratio

Figure 3.2 defines the cross section and the strain and stress conditions in a bonded section for the condition where the tendon ruptures simultaneously with compression failure of the concrete. The derivation is for a rectangular section or a T-section with a single layer of prestressed reinforcement where the compression block is within the depth of the flange, that is, $a < h_f$.

If the total strain capacity of the tendon is denoted by ε_{pu}, then the amount of strain available for flexure, ε_f, is the total strain capacity less the strain used for prestressing, ε_{pe}, the strain used to decompress the concrete, ε_d, and any loss of strain capacity due to sustained loads, ε_{pr}. This relationship is given in Eq. (3-1).

$$\varepsilon_f = \varepsilon_{pu} - \varepsilon_{pe} - \varepsilon_d - \varepsilon_{pr} \qquad (3\text{-}1)$$

The strain compatibility from Fig. 3.2 allows determination of the c/d ratio in terms of the available strains. Therefore, by using similar triangles

$$\frac{c}{d} = \frac{\varepsilon_{cu}}{\varepsilon_{cu} + \varepsilon_{pu} - \varepsilon_{pe} - \varepsilon_d - \varepsilon_{pr}} \qquad (3\text{-}2)$$

Equilibrium on the cross section equates the tensile force in the tendon to the compressive force on the concrete. Hence,

$$0.85 f_c' \beta_1 cb = \rho b d f_{pu} \qquad (3\text{-}3)$$

where β_1 = 0.85 for concrete strengths up to 27.5 MPa (4000 psi), after which it is reduced at a rate of 0.05 for each 6.9 MPa (1000 psi) of strength in excess of 27.5 MPa (4000 psi) to a minimum value of 0.65.

Solving Eq. (3-3) for the balanced reinforcement ratio, $\rho = \rho_b$, where $\rho = A_p/bd$ is the prestress reinforcement ratio, gives

$$\rho_b = 0.85 \beta_1 \frac{f_c'}{f_{pu}} \frac{c}{d} \qquad (3\text{-}4)$$

Substituting the expression for c/d from Eq. (3-2) into Eq. (3-4) gives the balanced ratio in terms of material properties.

$$\rho_b = 0.85 \beta_1 \frac{f_c'}{f_{pu}} \frac{\varepsilon_{cu}}{\varepsilon_{cu} + \varepsilon_{pu} - \varepsilon_{pe} - \varepsilon_d - \varepsilon_{pr}} \qquad (3\text{-}5)$$

An examination of the strain components in Eq. (3-5) leads to a simplification. First, the strain loss due to sustained loads is nearly zero if the strain due to sustained load is less than 50% of the ultimate tensile strain and is recovered at the nominal strength condition. Second, the decompression strain, ε_d, is typically an order of magnitude less than the

flexural strain. Setting these two strain values to zero gives the following simplified definition for ρ_b.

$$\rho_b = 0.85\beta_1 \frac{f_c'}{f_{pu}} \frac{\varepsilon_{cu}}{\varepsilon_{cu} + \varepsilon_{pu} - \varepsilon_{pe}} \qquad (3\text{-}6)$$

The strain $(\varepsilon_{pu} - \varepsilon_{pe})$ represents the strain available for flexure in the tendon. FRP tendons have ultimate strains ranging from 1.3 to 3.8% (Table 2.2). Assuming that 40 to 50% of the strain capacity remains after prestressing, there is 0.006 to 0.019 strain capacity available in the FRP tendon to allow the flexural member to deform and crack before failure. This reserve provides substantial deflection, thereby giving visual warning of overload conditions, and concrete cracking occurs at 0.002 net tensile strain.

The effective strain ε_{pe} is known because the designer selects it, and the manufacturer provides the ultimate stress and strain capacity for the tendon. The designer does need to know the basis for the selection of these ultimate values because some manufacturers provide the mean ultimate stress and strain while others, typically Japanese manufacturers, provide a strength value equal to the mean less three standard deviations. Eventually, the industry will establish a standard for reporting that is consistent with the specified capacity reduction factors for FRP tendons. ACI 440.1R refers to the guaranteed tensile strength as mean strength less three standard deviations.

3.4—Flexural design and capacity prediction

3.4.1 *Bonded construction*—The flexural behavior of a beam may be described according to whether the critical section is a compression-controlled or a tension-controlled section. A compression-controlled section condition occurs when the reinforcement ratio ρ is greater than ρ_b and the concrete crushes with no failure of the tendons. When ρ is less than ρ_b, a tension-controlled section condition occurs as a result of rupture of the tendons before crushing of the concrete.

3.4.1.1 *Tension-controlled section:* $\rho \leq \rho_b$—For reinforcement ratios less than ρ_b, the beam strength is governed by the tensile strength of the tendon, and the section is described as tension-controlled. In this case, the concrete strain will not reach 0.003 at failure of the beam, and, strictly speaking, the use of the rectangular stress block assumption would not be valid. For sections with $0.5\rho_b < \rho < \rho_b$, however, the concrete stress distribution will be substantially nonlinear at failure and thus an equivalent rectangular stress distribution can be assumed. Further, studies of the nominal capacity of lightly reinforced beams ($\rho < 0.5\rho_b$), where the stress in the concrete approximates a linear stress distribution, indicate use of a rectangular stress block assumption produces less than 3% error compared to an elastic analysis of a cracked section (Dolan and Burke 1996). Therefore, nominal moment capacity of a tension-controlled section with a single layer of reinforcement is developed using strength design based on a rectangular stress block.

Summing moments about the compression centroid (Fig. 3.2) defines the nominal moment capacity as

$$M_n = \rho b d f_{pu}\left(d - \frac{a}{2}\right) \qquad (3\text{-}7)$$

where a is computed from equilibrium of forces on the cross section, giving

$$a = \frac{\rho d \, f_{pu}}{0.85 f_c'} \qquad (3\text{-}8)$$

Combining the value for a with the nominal moment equation provides a combined form for prediction of nominal moment capacity

$$M_n = \rho b d^2 f_{pu}\left(1 - \frac{\rho \, f_{pu}}{1.7 f_c'}\right) \qquad (3\text{-}9)$$

The nominal capacity of a section in which the prestressing tendons are not in a single layer is discussed in Section 3.4.2.

3.4.1.2 *Compression-controlled section:* $\rho \geq \rho_b$—In a beam with $\rho \geq \rho_b$, the concrete will fail in compression before failure of the tendon. The stress and strain compatibility is the same as in Fig. 3.2; however, the value of the tendon strain is not known. This condition is analyzed by locating a neutral axis, assuming a linear elastic tendon and a rectangular stress block for the concrete. This is done by defining the strain in the tendon, equilibrating the horizontal forces on the section, solving for the neutral axis location, and finally summing moments about the tendon location.

With this amount of reinforcement in the beam, the concrete will have developed a highly nonlinear stress-strain relation so that the use of an equivalent rectangular stress block is appropriate. The depth of the neutral axis, c, can be found by considering axial force equilibrium of the cross section

$$\rho b d f_p = 0.85 f_c' \, b \beta_1 c \qquad (3\text{-}10)$$

Because FRP tendons are linear elastic to failure, the stress in the tendon f_p is a function only of the modulus of elasticity and the strain in the tendon

$$f_p = \varepsilon_p E_p \qquad (3\text{-}11)$$

The flexural strain in the tendon can be determined from the strain diagram at failure using similar triangles

$$\varepsilon_f = \varepsilon_{cu}\frac{d - c}{c} \qquad (3\text{-}12)$$

The total strain in the tendon can be expressed as the sum of the flexural strain and the effective prestressing strain ε_{pe}

$$\varepsilon_p = \varepsilon_{pe} + \varepsilon_{cu}\frac{d - c}{c} \qquad (3\text{-}13)$$
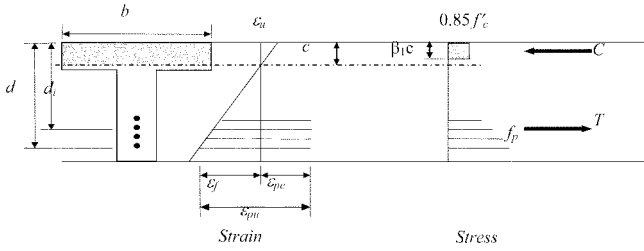
Note: Loss of strain capacity due to sustained load not shown

Fig. 3.3—Section with vertically distributed tendons.

Substitution of Eq. (3-13) and (3-11) into Eq. (3-10) and defining $k_u = c/d$ results in

$$\rho\left(\varepsilon_{pe} + \varepsilon_{cu}\frac{1-k_u}{k_u}\right)E_p = 0.85f_c'\beta_1 k_u \tag{3-14}$$

Defining a material constant λ such that

$$\lambda = \frac{E_p\varepsilon_{cu}}{0.85f_c'\beta_1} \tag{3-15}$$

and substituting Eq. (3-15) into Eq. (3-14) allows the resulting quadratic equation to be solved for k_u, giving

$$k_u = \sqrt{\rho\lambda + \left(\frac{\rho\lambda}{2}\left(1 - \frac{\varepsilon_{pe}}{\varepsilon_{cu}}\right)\right)^2} - \frac{\rho\lambda}{2}\left(1 - \frac{\varepsilon_{pe}}{\varepsilon_{cu}}\right) \tag{3-16}$$

The nominal moment capacity can be determined by summing moments about the tendon centroid, giving

$$M_n = 0.85f_c'\,b\beta_1 k_u d^2\left(1 - \frac{\beta_1 k_u}{2}\right) \tag{3-17}$$

3.4.2 *Development of flexural capacity for vertically distributed tendons in an under-reinforced section*—The above derivations assume that the prestressing tendons are all located at the same depth from the compression face. A method for determining the strength of vertically aligned tendons, based on the stress and the strain distribution, shown in Fig. 3.3, is presented in this section (Dolan and Swanson 2002).

The analysis is developed for a T-section with the assumption that the neutral axis is in the flange. Strain due to decompression of the concrete is small and has been neglected. Strains due to elastic and nonelastic shortening of the member are neglected as these strains are regained at the maximum curvature.

All tendons are assumed to be stressed to the same level f_{pe} and thus the stress increase at failure in the bottom tendon may be defined as $f_m = f_{pu} - f_{pe}$. Failure of the bottom tendon by rupture will lead to failure of the other tendons. The stress in each tendon can be determined from its strain, which can be expressed as a ratio of the strain at any level to the strain in the bottom tendon.

$$f_i = f_{pe} + f_m\frac{d_i - c/d}{d - c/d} = f_{pe} + f_m\left(\frac{\dfrac{d_i}{d} - \dfrac{c}{d}}{1 - c/d}\right) \tag{3-18}$$

where d_i is the depth of each individual tendon, and d is the depth of the bottom tendon.

Defining the initial prestress ratio $\xi = (f_{pe}/f_{pu})$ and $c = kd$, and assuming $\rho_i = (A_{pi}/bd)$ is the reinforcement ratio at level i, it can be shown that

$$k = \frac{\sqrt{\left(n\sum_{i=1}^{m}\rho_i\right)^2 + 2(1-\xi)n\sum_{i=1}^{m}\rho_i\left(\xi + \frac{d_i}{d}(1-\xi)\right)} - n\sum_{i=1}^{m}\rho_i}{1 - \xi} \tag{3-19}$$

where m is the number of layers of tendons.

Defining the depth ratio of the tendons as $\psi_i = (d_i/d)$ and assuming uniformly prestressed tendons, the moment capacity is

$$M_n = bd^2\sum_{i=1}^{m}\rho_i f_i\left(\psi_i - \frac{\beta_1 c}{2d}\right) \tag{3-20}$$

If the tendons through the depth of the member are prestressed to different levels, the nominal moment capacity is given as

$$M_n = bd^2\sum_{i=1}^{m}\left\{\rho_i\left[f_{pei} + f_m\left(\frac{\psi_i - c/d}{1 - c/d}\right)\left(\psi_i - \frac{\beta_1 c}{2d}\right)\right]\right\} \tag{3-21}$$

where f_{pei} is the effective prestress at the level i.

Most beams have a relatively small number of layers of tendons. Therefore, Eq. (3-20) and (3-21) are readily solved using a spreadsheet.

3.4.3 *Design implications of vertically distributed tendons*—Equations (3-20) and (3-21) provide a means to optimize the design of FRP prestressed beams. The prestressing ratio ξ may be varied at each depth so that the final stress distribution in the tendons is uniform with depth at maximum curvature. The reinforcement ratio may also be varied with depth to account for beams with mixed strand patterns such as harped strands and a large number of straight strands in the bottom flange.

3.4.4 *Unbonded construction*—For an unbonded prestressed member where strain compatibility between the concrete and the tendons cannot be assumed, the stress in the tendons at ultimate for an under-reinforced beam may be determined using the approach suggested by Naaman et al. (2002). This approach uses a strain-reduction coefficient Ω_u to relate the strain in an unbonded tendon to that in an equivalent bonded tendon. Knowing the strain in the tendons, the moment capacity may be computed as above for a bonded section. A description of this approach is given in Section 7.1. Bakis et al. (2001) applied this approach in beams post-
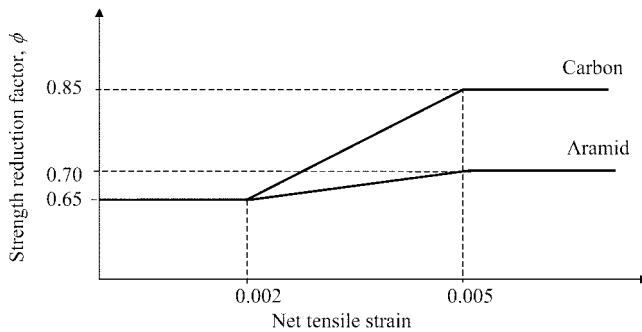
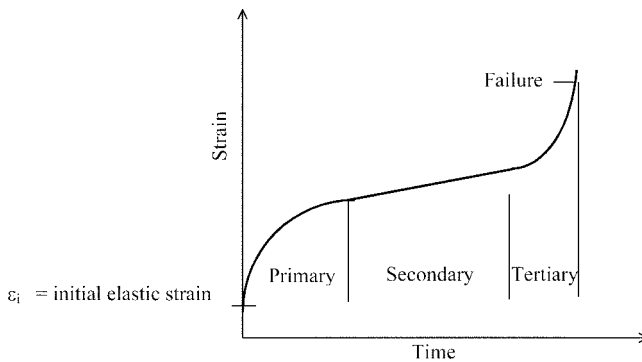Fig. 3.4—Variation in strength reduction factor with net tensile strain.

Fig. 3.5—The three stages of creep deformation.

Table 3.1—Recommended strength reduction factors (Dolan and Burke 1996)

Tendon type	Strength reduction factor ϕ	Condition
Aramid	0.70	Tension-controlled behavior
Carbon	0.85	
Aramid or carbon	0.65	Compression-controlled behavior

Table 3.2—Allowable concrete stresses

Allowable stress at transfer of prestress (before losses)	Units, MPa (psi)
(a) Extreme fiber stress in compression	$0.6f'_{ci}$ $(0.6f'_{ci})$
(b) Extreme fiber stress in tension except for (c)	$0.25\sqrt{f'_{ci}}$ $(3\sqrt{f'_{ci}})$
(c) Extreme fiber stress in tendon at ends	$0.5\sqrt{f'_{ci}}$ $(6\sqrt{f'_{ci}})$
Allowable stresses under service loads (after losses)	Units, MPa (psi)
(a) Extreme fiber stress in compression due to prestress plus sustained loads	$0.45f'_c$ $(0.45f'_c)$
(b) Extreme fiber stress in compression due to prestress plus total loads	$0.6f'_c$ $(0.6f'_c)$
(c) Extreme fiber stress in precompressed tensile zone	$0.5\sqrt{f'_c}$ $(6\sqrt{f'_c})$

Table 3.3—Allowable tendon stresses at jacking

Allowable jack stresses	
Carbon	$0.65f_{pu}$
Aramid	$0.50f_{pu}$
Allowable stress immediately following transfer	
Carbon	$0.60f_{pu}$
Aramid	$0.40f_{pu}$

tensioned with unbonded CFRP tendons, and obtained acceptable correlation between predicted and measured load-deflection relationships.

3.5—Strength reduction factors for flexure

The experimental strength from flexural tests on members prestressed with FRP tendons reported in the literature was compared to the strength predicted by the previous equations by Dolan and Burke (1996). The analysis of strength-reduction factors examined tendon type and failure mode. The strongest correlation was to tendon type. Capacity reduction factors for aramid and carbon tendons are presented in Table 3.1. ACI 440.1R recommends different capacity reduction factors for nonprestressed reinforcement. In that case, however, the reinforcement is predominately glass fibers. Thus, there is a consistent philosophy that performance is tied to reinforcement materials.

ACI 318-02 presents a unified approach to variation in strength reduction factors based on net tensile strain in the reinforcement. In keeping with this philosophy, a transition zone between tension-controlled and compression-controlled sections is presented. Tension-controlled sections have a net tensile strain, strain in the reinforcement farthest from the compression face, greater than or equal to 0.005, while compression controlled-sections have a net tensile strain less than or equal to 0.002. The transition in strength reduction factor is indicated in Fig. 3.4.

3.6—Flexural service stresses

Concrete service load stresses are the same as specified by the AASHTO Standard Specification for Highway Bridges

and are given in Table 3.2. These values are the same as ACI 318-02, except that the limitations on the tensile stresses in the concrete are more restrictive. Construction to these limits meets the requirements for a Class U member in ACI 318-02.

3.7—Jacking stresses

Steel tendons are typically stressed to 85% of their yield stress or approximately 0.005 strain. Allowable stresses in FRP tendons are typically limited to 40 to 65% of their ultimate strength due to stress-rupture limitations (Dolan et al 2000). This lower range of allowable stress actually corresponds to strains between 0.008 and 0.012, or 1.5 to 2.5 times the typical prestressing strain used in steel tendons. The recommended maximum jacking stresses for FRP tendons are given in Table 3.3. These stress limitations, which are based on creep-rupture characteristics of the tendons, should not exceed 65% of the maximum stress that can be developed when tested using the anchorage specified by the manufacturer.

3.8—Creep rupture of FRP tendons

Creep is the inelastic strain of a material under a sustained load over a period of time. Creep rupture is the tensile fracture of a material subjected to sustained high stress levels over a period of time. There are three stages of creep: primary, secondary, and tertiary, as shown in Fig. 3.5. The primary stage, characterized by a continually decreasing strain rate, confined to a short time (relative to creep rupture time) immediately following application of load, is common for
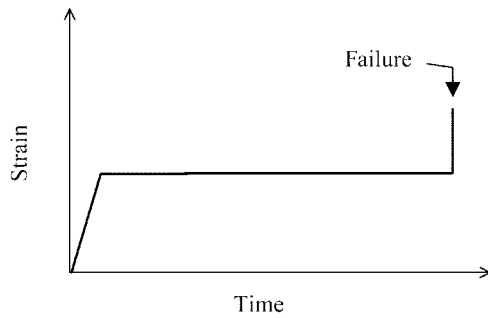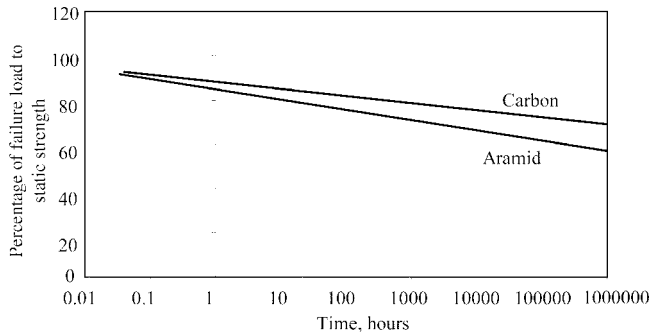
Fig. 3.6—Carbon creep-rupture curve.

Fig. 3.7—Comparison of creep-rupture curves for aramid and carbon FRP rods under environmental exposure.

FRP composites. The second stage is defined as the time period in which the strain rate is constant under constant stress. In this period, some of the weaker fibers may fail, but the friction or resin adhesion between the fibers transfers the load to adjacent fibers. If the stress level is low enough, fiber damage is confined to the secondary creep level, and the tendon has an unlimited service life. The tertiary stage, characterized by an increasing strain rate, represents rapid, progressive failure of the fibers until the tendon ruptures.

The creep strain behavior of AFRP tendons typically follows the three stages of creep: primary, secondary, and tertiary (Fig. 3.5). The strain rate of CFRP tendons during the secondary stage drops to zero. These tendons exhibit near-instantaneous failure compared to the secondary stage when the initial stress level exceeds the creep-rupture threshold (Fig 3.6).

Designers need to know the limiting percentage of ultimate load that may be applied to a tendon so that the tertiary stage is never reached. If the creep in the secondary stage is small, an equilibrium condition will be achieved and the material becomes stable.

Figure 3.7 shows the extrapolation of creep-rupture data obtained by Dolan et al. (2000) for aramid and carbon tendons encased in concrete surrounded by saltwater and subjected to a constant load. This figure shows the time to failure of the FRP tendon as a function of applied load in the tendon.

The creep-rupture curves provide allowable prestress levels for AFRP and CFRP rods for any given service life. The predicted stress level for CFRP is 70% of the tendon's short-term ultimate strength for 100 years of service. The upper limit of service load at a 100-year life for AFRP is predicted to be 55% of the tendon's short-term ultimate strength in a concrete environment.

The curves in Fig. 3.7 were extrapolated from experimental data obtained from tests conducted for over 12,000 h that used applied loads between 50 to 80% of the ultimate load. At conclusion of the tests, all unbroken tendons were tested to failure. The residual strength of the CFRP was 90% of its original static capacity, while that of the AFRP was 80% of its original capacity.

3.9—Correction of stress for harped tendons

FRP tendons behave linearly elastically to failure. Consequently, draping or harping of tendons results in a loss of tendon strength in the vicinity of the harping or draping points due to increased strain induced by curvature of the tendons. When the FRP tendon is deflected, the jacking stresses should be reduced to account for localized stress increases. Dolan et al. (2000) proposed that the stress increase due to harping, in solid and stranded tendons, can be defined by the following equation

$$f_h = \frac{E_f R_t}{R} \tag{3-22}$$

where E_f is the modulus of elasticity of the fiber; R_t is the radius of the tendon; and R is the radius of curvature of the harping saddle.

The combined stress in a tendon of cross-sectional area, A_p, at a harping saddle, due to the jacking load P_j, is given by Eq. (3-23) and should be less than the allowable stress values

$$f = \frac{P_j}{A_p} + \frac{E_f R_t}{R} \tag{3-23}$$

3.10—Relaxation and friction losses

Relaxation losses (*REL*) in FRP tendons results from three sources: relaxation of polymer R_p; straightening of fibers R_s; and relaxation of fibers R_f. The total relaxation loss, $REL = R_p + R_s + R_f$, expressed as a percentage of the stress at transfer, can be estimated by assessing these three effects separately:

Relaxation of polymer R_p—When the tendon is initially stressed, a portion of the load is carried in the resin matrix. Over time, the matrix relaxes and loses its contribution to the load-carrying capacity. This initial matrix relaxation occurs within the first 24 to 96 h and may be accelerated by heat curing of prestressed concrete beams (Dolan et al. 2000). This relaxation is affected by two characteristics of the tendon: the modular ratio of the resin to the fiber, n_r, and the volume fraction of fibers in the tendon, v_f. The modular ratio n_r is defined as the ratio of the elastic modulus of the resin, E_r, to the modulus of the fiber, E_f. The relaxation loss is the product of the volume fraction of resin, $v_r = 1 - v_f$, and the modular ratio of the resin n_r, giving

$$R_p = n_r \times v_r$$

For resins used in pultrusion operations, the modular ratio is approximately 1.5% for carbon and 3% for aramid. The resin volume fraction is typically 35 to 40% of the tendon cross section. Therefore, the total relaxation in the first phase is in the range 0.6 to 1.2% of the transfer stress. This relaxation loss can be compensated by overstressing, as long as the total stress limits given in Table 3.3 are not exceeded. Overstressing and allowing the relaxation to reduce the stress to the values given in Table 3.3 is not recommended because the loss does not occur in the fibers and the fibers would be permanently overstrained.

Straightening of fibers R_s—The fibers in a pultruded section are nearly, but not completely, parallel. Therefore, stressed fibers flow through the matrix and straighten, and this straightening appears as a relaxation loss. Straightening of the fibers is a function of the quality control of the pultrusion process. A 1 to 2% relaxation is adequate to predict this phase of the loss calculation (Dolan et al. 2000).

Relaxation of fibers R_f—Fiber relaxation is dependent on the fiber type. Carbon fibers are reported to have no relaxation; therefore, R_f for carbon may be assumed to be zero. Aramid materials creep when loaded, and this creep behavior is reflected in its relaxation behavior. The long-term relaxation for Kevlar™ fibers has been reported by DuPont to be 1 to 3% per decade on a log scale. By assuming that the relaxation count begins after the first 24 h, the total relaxation for aramids can be assumed to be 6 to 18% in a 100-year design life (Dolan 1989).

Zoch et al. (1991) performed relaxation tests on CFCC and steel strands under equivalent conditions. Strands of both materials with 12.5 mm diameter were prestressed to 80% of their proof load, and relative decrease in load over time was measured. The results showed that over a period of 100 h, the stress was reduced by 2% for CFCC, whereas steel relaxed approximately 8% from the original load. This indicates a superior relaxation resistance of CFCC to permanent stress. Santoh (1993) conducted relaxation tests on CFCC and steel strands at room temperature. They found that at 50% of the ultimate stress, the relaxation value after 100 h for CFCC was 0.48% and was 1.02% for steel; at 65% of the ultimate stress, the relaxation of CFCC was 0.81%, while that of steel was 2.28%. At 80% of the ultimate stress, it was 0.96% for CFCC and 7.35% for steel. They concluded from their tests that the relaxation of CFCC is 50% or less than that of steel.

In assessing friction loss, relevant curvature friction and wobble coefficients should be used. Such data are sparse. Burke, Nelson, and Dolan (2000) found that, for a CFRP tendon in a PVC duct, the curvature friction coefficient could range from 0.25 for stick-slip (dynamic) behavior to 0.6 for no-stick-slip (static) behavior. Because the wobble coefficient relates primarily to the type of duct, values specified for steel prestressing systems with plastic ducts may be applied to FRP tendons.

Traditional losses associated with prestressing tendons, such as friction, initial elastic shortening, and concrete creep and shrinkage, can be computed in the same manner as for prestressed steel tendons. Relevant friction and wobble coefficients should be obtained from the manufacturer of the prestressing system used.

3.11—Overall design approach

The overall design approach for FRP prestressing tendons is to use the equations for flexural behavior to establish the tendon size to meet the strength requirements of the section. A prestress level of 40 to 50% of the tendon strength is selected for the initial prestress force, and service level stresses are checked. If the section is sufficient, the flexural design is completed. If it is not, the number or size of the tendons is increased or the section size adjusted to meet service requirements, and then the strength capacity is rechecked. Nonprestressed FRP reinforcement may be used to increase the strength of a section.

3.12—Ductility or deformability

FRP tendons and concrete are both brittle materials; therefore, classical ductility, which requires plastic deformation, is difficult to obtain. Possible ways to obtain quasiductile behavior, even with brittle materials, are by confining the concrete in compression, partial prestressing, or permitting some bond slip. If ductility is defined as the energy absorbed, then the small area under a FRP prestressed load-deflection curve suggests that energy absorption ductility is limited (Naaman and Jeong 1995). Grace and Abdel-Sayed (1998a), however, have demonstrated that the ductility of a CFRP prestressed concrete beam can be enhanced by combining bonded internal and unbonded externally draped tendons. Conversely, deformability may be defined as the ratio of deflection at ultimate to deflection at cracking. Using the latter definition, FRP prestressed members can have considerable deformability.

Deformability is a key issue in determining the safety of FRP prestressed structures. Because FRP tendons do not exhibit ductility under the traditional definition, care should be taken to ensure that sufficient warning is exhibited before failure. Due to the lack of ductility, the concept of deformability as an index to measure performance provides a method of ensuring that this warning exists. Several approaches have been taken to quantify this concept into a deformability index (Mufti, Newhook, and Tadros 1996). This is usually accomplished through a ratio of deflections or curvatures under ultimate loads to those same quantities under service loads. The deformability index is intended to be a design check and not a long and complicated design procedure.

The use of an ultimate deflection-to-service-deflection ratio gives an indication of the warning to failure, but there are two main difficulties with this approach. The first issue is that deflections for point loads or uniform loads on a simple span beam are simple to calculate, but deflections for continuous structures with various loads require rigorous analysis or the use of a computer analysis program. The second issue is the difficulty in determining the deflection under ultimate loads. Traditional approaches to calculating deflections for concrete members consider the softening effect due to cracking under service loads. Near ultimate loads, this softening occurs at a faster rate and is harder to quantify.

An alternative approach is to use a ratio of the curvatures at ultimate and service loads. This is more easily accomplished by using quantities already calculated during the design process. The formula for this approach to the deformability index, DI, is shown in Eq. (3-24) (Dolan and Burke 1996).

$$\text{DI} = \frac{(1-k)}{\left(1 - \frac{\alpha}{d\beta_1}\right)} \frac{\varepsilon_{pu}}{\varepsilon_{ps}} \qquad (3\text{-}24)$$

where $\alpha = \rho df_{pu}/0.85f_c'$.

If service loads are considered as the load to produce a tensile stress in the concrete of $0.25\sqrt{f_c'}$ MPa ($3\sqrt{f_c'}$ psi), the decompression strains and the strain to produce $0.25\sqrt{f_c'}$ MPa ($3\sqrt{f_c'}$ psi) are very small compared to the prestress strain. The index is effectively a function of the ratio of ultimate strain to the prestressing strain with a slight modification due to the differences in the neutral axis of elastic and inelastic behavior.

It follows from this definition that the most efficient method to obtain high deformability is to reduce the initial FRP tendon strain, which provides more tendon strain reserve, greater curvature or deflection capacity, and a higher index. A ratio of ultimate to initial prestress strain is easier to compute than the deformability index and provides similar results. Limiting the initial jacking stress to the values given in Table 3.3 results in acceptable deformability.

3.13—Minimum reinforcement

The amount of prestressed and nonprestressed reinforcement should be adequate to develop a factored flexural resistance ϕM_n greater than the smaller of 1.5 times the cracking strength or, for a tension-controlled section, 1.5 times the moment due to factored loads (CAN/CSA S806).

CHAPTER 4—SERVICABILITY
4.1—General

The allowable stresses specified in Table 3.2 ensure that the tensile strength of the concrete will not be exceeded and members will meet the ACI 318-02 requirements for Class U. It is still necessary, however, to ensure that the deflection, both short- and long-term, is acceptable for end use of the member.

4.2—Deflection

4.2.1 *Short-term deflection*—Deflections for FRP prestressed beams can be divided into two categories: short-term and long-term deflections. Before cracking, the gross moment of inertia can be used to calculate the deflections from traditional mechanics of materials. If deflection calculation following crack formation is required, methods that take into account the softening effect that cracking has on concrete members need to be used. This can be accomplished using a modified effective moment of inertia, I_e, proposed by ACI 440.1R and given by Eq. (4-1)

$$I_e = \left(\frac{M_{cr}}{M_a}\right)^3 \beta_d I_g + \left(1 - \left(\frac{M_{cr}}{M_a}\right)^3\right) I_{cr} \leq I_g \qquad (4\text{-}1)$$

in which β_d is a factor to soften the effective moment of inertia and is

$$\beta_d = 0.5\left[\frac{E_p}{E_s} + 1\right]$$

where E_p is the modulus of elasticity of FRP tendon; E_s is the modulus of elasticity of steel; I_g is the gross moment of inertia; M_{cr} is the cracking moment; M_a is the maximum moment in a member at which the deflection is being computed; and I_{cr} is the cracked moment of inertia, which, for a rectangular section or a flanged section with $kd < h_f$, can be calculated from Eq. (4-2).

$$I_{cr} = \frac{b(kd)^3}{3} + nA_p(d - kd)^2 \qquad (4\text{-}2)$$

In Eq. (4-2), the parameter k may be found from Eq. (3-19). If the reinforcement is in a single layer $i = 1$ and $d_1 = d$. This approach is valid for loads between cracking of the concrete and up to around 50% of the ultimate load.

Subsequent to cracking, deflection due to specified live load should be calculated as the difference between the deflection due to the total service load and the deflection due to dead load. This bilinear approach is the same as recommended by PCI (2000). The deflection is not only due to the change of the effective moment of inertia I_e, but also due to the change of the eccentricity of the prestressing force after cracking. Abdelrahman and Rizkalla (1998) have suggested modifications to account for the change in effective eccentricity by finding the effective neutral axis location

$$y_{eff} = \left(\frac{M_{cr}}{M_a}\right)^2 y_g + \left(1 - \left(\frac{M_{cr}}{M_a}\right)^2\right) y_{cr} \qquad (4\text{-}3)$$

where y_{eff} is the distance from the extreme compression fiber to the effective neutral axis; y_g is the distance from the extreme compression fiber to the centroid of the gross section; and y_{cr} is the distance from the extreme compression fiber to the neutral axis of the cracked section (that is, kd).

4.2.2 *Long-term deflection*—For long-term deflections, camber and deflection are separated into individual components, adjusted by a multiplier, and then superimposed to obtain final deflections in a manner similar to that for conventional steel prestressed concrete members (PCI 2000). The multipliers for FRP prestressed concrete for predicting long-term deflections, as suggested by Currier (1995), are shown in Table 4.1. These values are based on one series of experimental data consisting of three beams with each tendon type. The change in concrete strain over a period of approximately 1 year has been documented by Grace (2000a) for DT girders prestressed with CFRP tendons. Research on the long-term loss of prestress and resultant time-dependant camber/deflection effects is needed to define the time-dependant deflection relationship of concrete members prestressed by FRP tendons. Alternatively, the multiplier method of Kelly, Bradberry, and Breen (1987) may be used to calculate

Table 4.1—Suggested multipliers for FRP tendons

		Without composite topping	
		Carbon	Aramid
At erection	Deflection due to self-weight	1.85	1.85
	Camber due to prestress	1.80	2.00
Final	Deflection due to self-weight	2.70	2.70
	Camber due to prestress	1.00	1.00
	Deflection due to applied loads	4.10	4.00

camber and deflection, if the time-dependant loss of prestress for a chosen FRP tendon is known, or assumed, along with the time-dependant concrete properties.

The multipliers in Table 4.1 are for members without composite toppings. The *PCI Design Handbook* (PCI 2000) indicates that multipliers relating to final deflection for topped members are smaller than for members without composite topping. Consequently, the use of values in Table 4.1 should be conservative for topped members.

4.3—Crack width and spacing

Dolan et al. (2000) studied crack widths in flexural members prestressed with CFRP. Both monotonic and cyclic loadings were studied. A linear growth in crack width with increasing load was observed after the initial precompression was overcome. The cracks were evenly spaced and occurred at the location of the stirrups, suggesting that major debonding of the carbon tendons did not occur during static or fatigue loading. Initial crack width was correlated with the Gergely-Lutz crack width equation when corrected by scaling the stress term by the ratio of the modulus of elasticity of steel to that for the FRP tendons. Crack lengths and widths increased during flexural cycling. Final crack widths were approximately three times those in a comparable steel prestressed concrete beam.

4.4—Fatigue

It is unlikely that fatigue will be a problem in uncracked members as the stress range in the tendons under repeated loading will be small (Grace 2000b; and Grace, Enomoto, and Yagi 2002). Further, Dolan et al. (2000) have shown that cracked CFRP prestressed concrete beams showed no fatigue failure after 3,000,000 flexural cycles with nominal tensile stresses of 0.5 $\sqrt{f_c'}$ MPa (6 $\sqrt{f_c'}$ psi) at the extreme fiber of the beams. Cracking was observed after the first 100,000 load cycles. Gradual softening was observed, but the beams indicated no loss of strength due to the fatigue loading.

A forensic examination of the beams after static loading to failure indicated that the tendons failed in tension, as evidenced by the "straw broom" failure shown in Fig. 4.1. Because all the carbon tendons failed in tension at close to the predicted strength, it can be assumed that the full tensile strength of the tendon was developed (the flexural cycling had no effect on the tensile strength of the tendon). An investigation of the saddle for the harping point indicated some evidence of sliding contact between the tendons and the

Fig. 4.1—Carbon tendon after "straw broom" failure.

Fig. 4.2—Friction evidence on saddle.

saddle during cycling, as shown in Fig. 4.2; however, no significant fraying of the tendons was visible. There was evidence of contact near the edge of the saddle. It is recommended that a small radius be turned on the edges of any production saddle to minimize possible edge or bending effects.

CHAPTER 5—SHEAR

The use of FRP as shear reinforcement in beams prestressed with FRP tendons has not been thoroughly investigated (Fam, Rizkalla, and Tadros 1997; Shehata 1999). From the assessment of theoretical and experimental nominal shear capacities, a rational approach that conservatively modifies the ACI 318-02 expressions to account for the special characteristics of FRP stirrups is suggested.

5.1—General considerations in design of FRP stirrups

Because of differences between FRP and steel, several issues need to be addressed when using FRP as shear reinforcement, namely:
- FRP may have a relatively low modulus of elasticity;
- FRP has high tensile strength and no yield plateau;
- Tensile strength of the bent portion of an FRP bar is significantly lower than the straight portion;

- FRP has lower dowel resistance and tensile strength in any direction other than that of the fibers; and
- The bond characteristics of FRP stirrups may vary significantly from steel reinforcement.

5.2—Shear strength with FRP stirrups

According to ACI 318-02, the nominal shear strength of any concrete cross section, V_n, is considered as the sum of the shear resistance provided by concrete, V_c, the shear resistance provided by stirrups, V_s, and the shear resistance provided by the vertical component of prestressing force, V_p.

Members prestressed with FRP tendons behave similarly to members prestressed with steel tendons. The nominal shear resistance V_n is given by

$$V_n = V_c + V_{frp} + V_p \qquad (5\text{-}1)$$

The following formulation for V_c is suggested

$$V_c = 0.17\sqrt{f_c'}\,b_w d \ \text{N} \quad (2.0\sqrt{f_c'}\,b_w d \ \text{lb}) \qquad (5\text{-}2)$$

The ACI code provides several alternative formulations for the concrete contribution to shear resistance. A search of the literature on the shear strength of FRP prestressed beams found information on only a small number of samples in which there was a significant variation in specimen size and tendon type (Dowden and Dolan 1997). This paucity of test data, together with the fact that wider shear cracks, which will probably occur in a beam prestressed with FRP rather than steel tendons, does not warrant expansion of V_c beyond the minimum value specified in Eq. (5-2) at this time.

A similar approach to account for the contribution of FRP stirrups has been taken. The shear resistance provided by FRP stirrups, V_{frp}, when the stirrups are vertical can be written as

$$V_{frp} = \frac{f_{fb} A_v d}{s} \qquad (5\text{-}3)$$

and

$$f_{fb} = \phi_{bend} f_{fu} \qquad (5\text{-}4)$$

where the value of ϕ_{bend} is as follows

$$\phi_{bend} = \left(0.11 + 0.05\frac{r}{d_b}\right) \text{ and } 0.25 \le \phi_{bend} \le 1.0 \qquad (5\text{-}5)$$

where r is the radius of the bend.

The maximum stress in the FRP reinforcement is limited to the smaller of 0.002 times the modulus of elasticity of the stirrup, or the strength of the bent portion of the stirrups $\phi_{bend} f_{fu}$.

The form of Eq. (5-3) is the same as that given in ACI 318-02, except f_y is replaced by a stress in the FRP rod based on its r/d_b, as shown in Eq. (5-4). The parameter ϕ_{bend} (Eq. (5-5))

is modified from the original JSCE (1997) formulation so that the minimum reduction factor is limited to 0.25. This was based on the push-apart tests performed on the aramid/nylon and carbon/nylon stirrups, which resulted in a ϕ_{bend} of 0.25 (Currier 1995). Also, in the equation for the design stress of the FRP stirrups provided in JSCE (1997), the factor 0.3 has been reduced to 0.11. Moreover, the modified expression for ϕ_{bend} is more conservative than the form suggested in JSCE (1997); consequently, Eq. (5-5) is suitable for design applications until more refinement of the r/d_b response is available.

5.3—Spacing limits for shear reinforcement

ACI 318-02, Section 11.5.4, guards against excessive crack width by limiting the maximum spacing of shear reinforcement for prestressed members to $0.75h$ or 600 mm (24 in). The maximum stirrup spacing is reduced to half of this when the maximum shear V_{frp} exceeds $0.33\sqrt{f_c'}\,b_w d$ N $(4.0\sqrt{f_c'}\,b_w d \ \text{lb})$. The Canadian Highway Bridge Design Code limits the tensile strain in FRP shear reinforcement to 0.002. These two conditions ensure that cracks are relatively small and uniformly distributed in the member. For FRP stirrups, the maximum spacing should be limited to $d/2$ or 600 mm (24 in.) as suggested by ACI 318-02 for nonprestressed members.

5.4—Minimum amount of shear reinforcement

ACI 318-02 requires a minimum amount of shear reinforcement when V_u, the factored shear force at a section, exceeds $\phi V_c/2$. This requirement is to prevent shear failure in members where the sudden formation of cracks can lead to excessive distress (Joint ACI-ASCE Committee 426 1973). Equation (5-6) gives the recommended minimum amount of shear reinforcement for FRP members.

$$A_{v,\,min} = \frac{1}{16}\sqrt{f_c'}\,\frac{b_w s}{\phi_{bend} f_{fu}} \quad (\text{mm}^2) \qquad (5\text{-}6)$$

$$\text{or } A_{v,\,min} = 0.75\sqrt{f_c'}\,\frac{b_w s}{\phi_{bend} f_{fu}} \quad (\text{in.}^2)$$

The expression is a modification to ACI 318-02, Section 11.5.5.3. It uses the effective strength of the stirrup at the bends instead of the yield strength of reinforcing steel to conservatively estimate the minimum amount of stirrups. The value of $\phi_{bend} f_{fu}$ should not exceed 0.002 times the modulus of elasticity of the stirrup.

5.5—Detailing of shear stirrups

Limited experimental data are available on bond behavior of the bent portion of FRP stirrups. ACI 318-02 provisions for bond of hooked steel bars cannot be applied directly to FRP reinforcing bars because of their different mechanical properties. Research on FRP hooks (Ehsani, Saadatmanesh, and Tao 1995) indicates that the tensile strength of the bent portion of a GFRP bar is mainly influenced by the ratio of the bend radius to the bar diameter, r/d_b, the tail length, and to a
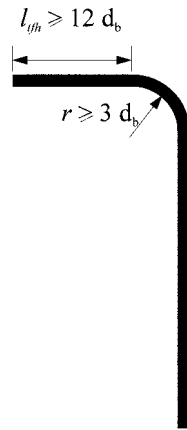
Fig. 5.1—Minimum radius and tail length of a stirrup bend.

lesser extent, the concrete strength. Tests by Ehsani, Saadatmanesh, and Tao (1995) indicated that for specimens with r/d_b of zero, the reinforcing bars failed in shear at very low load levels at the bends. Therefore, although manufacturing of FRP bars with sharp bends is possible, such details should be avoided due to the low shear strength of FRP bars. As indicated by Ehsani, Saadatmanesh, and Tao (1995), a minimum r/d_b of 3 is recommended. In addition, FRP stirrups should be closed stirrups with 90-degree hooks. The tensile force in a vertical stirrup leg is transferred to the concrete through the tail beyond the hook as shown in Fig. 5.1. Ehsani, Saadatmanesh, and Tao (1995) found that for a tail length l_{tfh} beyond $12d_b$, there is no significant slippage and no influence on the tensile strength of the stirrup leg. Therefore, it is recommended that a minimum tail length of $12d_b$ be used.

CHAPTER 6—BOND AND DEVELOPMENT
6.1—Introduction

The transfer and development length of an FRP tendon is a function of the configuration of the perimeter and the surface condition of the FRP, the stress in the FRP, the method used to transfer the FRP force to the concrete, and the strength and cover of the concrete. The mechanism of bond differs between FRP and steel strands due to differences in shapes, surface treatments, and elastic moduli. FRP may be produced using unique manufacturing processes, which result in different characteristic surface textures. In general, a prestressing rod with a rough, irregular surface will require a shorter transfer length than a smooth one. The transfer length will be greater if the release of tension is sudden rather than gradual. A higher initial prestress in the tendon will require a larger transfer length. In general, the bond of FRP tendons could be influenced by (ACI 440R):

- Tensile strength (600 to 3000 MPa [87,000 to 435,000 psi]);
- Modulus of elasticity (40 to 170 GPa [5.8×10^6 to 25×10^6 psi]);
- Hoyer effect;
- Cross-sectional shape;
- Surface preparation (braided, deformed, smooth);
- Type and volume of fiber and matrix;
- The method of force transfer; and
- Concrete strength and cover.

Both transfer length and development length vary considerably among the different fibers and tendon configurations. This variation is discussed in the following sections.

6.2—Transfer length

The transfer length in pretensioned concrete is the minimum length required to transfer the full prestressing force to the concrete. This transfer occurs gradually, rising from zero at the location where bond is initiated and increasing gradually within the transfer length until it reaches a constant value at the effective prestress level.

6.2.1 *Aramid FRP*—Nanni et al. (1992) examined the transfer length of FiBRA tendons comprising braided epoxy-impregnated AFRP and having diameters ranging from 8 to 16 mm (5/16 to 5/8 in.). Their experimental transfer lengths ranged from 300 to 400 mm (12 to 16 in.) for low levels (25% of ultimate) of prestress and from 250 to 550 mm (10 to 22 in.) for high levels (50% of ultimate) of prestress. The transfer length values varied with the nominal diameter of the different tendons and ranged from 30 to 40 strand diameters. The authors concluded that friction was the predominant bonding mechanism in aramid fibers and that these fibers showed little tendon slippage compared to steel.

Taerwe and Pallemans (1995) carried out a study on Arapree® aramid fiber rods having diameters of 7.5 and 5.3 mm (0.3 and 0.2 in.) and different surface finishes. They suggested a transfer length of 16 times the nominal diameter for Arapree® rods.

Ehsani, Saadatmanesh, and Nelson (1997) conducted tests on Arapree® (10 mm [0.39 in.]), FiBRA (10.4 mm [0.41 in.]), and Technora (7.4 mm [0.29 in.]) tendons. The transfer length was found to be 33 bar diameters for FiBRA, 43 bar diameters for Technora®, and 50 bar diameters for Arapree.® For Arapree® tendons, the transfer length was affected significantly by the level of prestress.

Lu et al. (2000) conducted transfer length tests on Technora (7.9 mm [0.31 in.]) aramid/vinylester tendons. The transfer lengths varied between 45 to 47 diameters during tendon release, immediately after full tendon release, and 90 days following full release. In consideration of other types of FRP tendons tested by Lu et al. (2000), a minimum transfer length of 50 times the strand diameter was recommended.

6.2.2 *Carbon FRP*—Domenico (1995) investigated the transfer length and bond characteristics of CFCC strands. Variables in the study were the depth of the beams, diameter of the CFCC tendons, concrete covers and strength, and prestressing level. The measured transfer length was found to be proportional to the diameter of the CFCC strand and the prestress level, and varied from 140 to 400 mm (5.5 to 15.7 in.).

Mahmoud and Rizkalla (1996), and Mahmoud, Rizkalla, and Zaghloul (1997) studied the bond characteristics of Leadline™ and CFCC strands. The authors reported that the measured transfer length varied from 450 to 650 mm (17.7 to 25.6 in.) or 56 to 81 bar diameters for Leadline™ rods, and from 300 to 425 mm (11.8 to 16.7 in.) for CFCC strands. They recommended Eq. (6-1) for transfer length of carbon FRP.

Table 6.1—Typical transfer and development lengths for FRP tendons

Material	Type	Diameter, mm (in.)	Young's modulus, MPa (ksi)	Tensile strength, MPa (ksi)	f_{pe}/f_{pu}	L_t/d_b	L_d/d_b
Aramid	Arapree®	9.9 (0.39)	127,600 (18,500)	2450 (355)	0.5 to 0.7	16 to 50	100
	FiBRA	10.4 (0.41)	48,270 (7000)	1430 (208)	0.4 to 0.6	20 to 50	90
	Technora®	7.4 (0.291)	68,600 (9950)	1720 (250)	0.6	50	140
Carbon	Leadline™	7.9 (0.312)	149,600 (21,700)	1980 (287)	0.5 to 0.7	50 to 80	175
	CFCC	8.3 (0.327)	137,200 (19,900)	2220 (322)	0.5 to 0.7	50	N/A

$$L_t = \frac{f_{pe}d_b}{\alpha_t f_c'^{0.67}} \qquad (6\text{-}1)$$

where α_t is 1.9 for N-mm units (10.0 for inch-pound units) for Leadline™, and 4.8 for N-mm units (25.3 for inch-pound units) for CFCC. Grace (2000a) found that α_t is 1.95 for N-mm units (10.2 for inch-pound units) for Leadline™ and 2.12 for N-mm units (11.2 for inch-pound) for CFCC, and suggested further study on the transfer length of CFCC strands.

Ehsani, Saadatmanesh, and Nelson (1997) conducted tests on Leadline™ and CFCC carbon tendons and found the transfer length to be 54 times the diameter for Leadline™ and 50 times the diameter for CFCC.

Soudki, Green, and Clapp (1997) reported on the transfer length for Leadline™ CFRP rods in concrete T-beams. They found that the measured transfer length was approximately 80 times the rod diameter, and that existing models for steel may give unconservative transfer lengths for the CFRP rod.

Lu et al. (2000) investigated single Leadline™ and generic carbon/epoxy tendons with 7.9 mm (0.31 in.) nominal diameter. The generic tendons had a shallow waffle-type of surface deformation applied during the pultrusion manufacturing process. Transfer lengths in the beams investigated were between 52 and 53 diameters for both tendons. A conservative value of transfer length equal to 50 times diameter was recommended for the tested CFRP tendons.

6.3—Flexural bond length

6.3.1 *Aramid FRP*—Nanni and Tanigaki (1992) examined the development and flexural bond lengths of AFRP tendons. The unfactored development length of AFRP tendons in bonded pretensioned prestressed concrete members was determined as: 120, 100, and 80 times the nominal diameter for type K64, K128, and K256 tendons, respectively.

Lu et al. (2000) found that the development length of single 7.9 mm (0.31 in.) diameter Technora® tendons could not be directly measured due to the concrete crushing or tendon slip failures in the beams investigated. By using an extrapolation procedure on the linear plots of tendon force at failure versus embedment length, however, the development length that would be required to fail the tendons in tension was determined to be 141 diameters. ACI 318-02 equations were determined to be overconservative in comparison with Lu et al.'s measurements. A recommended relationship for predicting the development length of single AFRP tendons was reported.

6.3.2 *Carbon FRP*—Ehsani, Saadatmanesh, and Nelson (1997) examined the transfer and flexural bond lengths of carbon and aramid FRP prestressing tendons. Two types of CFRP strands, Leadline™ and CFCC, and three AFRP types, Technora®, FiBRA, and Arapree® were tested. It was concluded that the ACI 318 development length requirements for steel strands are conservative for AFRP tendons but are not adequate for Leadline™ tendons.

Lu et al. (2000) found that the development length of single Leadline™ carbon/epoxy tendons and generic carbon/epoxy tendons (both 7.9 mm [0.31 in.] diameter) with a shallow waffle pattern could not be determined due to compressive failure in the concrete beams tested. Using an extrapolation procedure, maximum development lengths for tensile failure of the Leadline™ and generic tendons were determined to be 138 and 146 diameters, respectively. Lu et al. (2000) recommended Eq. (6-2), which predicted the development length of these CFRP tendons with good accuracy.

$$L_d = \frac{1}{3}f_{pe}d_b + \frac{3}{4}(f_{pu} - f_{pe})d_b \qquad (6\text{-}2)$$

Mahmoud and Rizkalla (1996) and Mahmoud, Rizkalla, and Zaghloul (1997) recommended the following equation for flexural bond of carbon FRP

$$L_{fb} = \frac{(f_{pu} - f_{pe})d_b}{\alpha_{fb} f_c'^{0.67}} \qquad (6\text{-}3)$$

where α_{fb} is 1.0 for N-mm units (5.3 for inch-pound units) for Leadline™ and 2.8 for N-mm units (14.8 for inch-pound units) for CFCC.

6.4—Design considerations

Bond and development for prestressing FRP tendons made of carbon or aramid fibers are intended to provide bond integrity for the strength of the member. Typical values for transfer and development lengths of various FRP tendons are given in Table 6.1.

Many of the bond tests were conducted with direct pullout tests (Nanni et al. 1992; Nanni and Tanigaki 1992). These tests indicated that failure of the tendon surface was the principal factor limiting bond capacity. Research at the University of Minnesota (Shield, French, and Hanus 1999) recorded cracking and splitting of the concrete. The body of experimental data, especially that from pullout tests, does not provide

sufficient information to define tendon spacing limitations or cover restrictions for FRP tendons. The designer should select spacing based on the specific tendon contemplated.

CHAPTER 7—UNBONDED AND EXTERNAL TENDON SYSTEMS
7.1—Unbonded prestressed members

To predict the strength of a beam post-tensioned with unbonded FRP tendons, it is necessary to determine the stress in the prestressing tendons at failure of the beam using the following relation

$$f_p = f_{pe} + \Delta f_p \qquad (7\text{-}1)$$

where f_{pe} is the effective prestress in the tendon when the beam carries only the dead load after the prestress losses have occurred, and Δf_p is the stress increase above f_{pe} due to any additional applied load. The inclusion of dead load and losses is important because, when computing prestress losses needed to determine the final value of the prestressing force, the dead load moment is considered active in estimating creep losses. There is no compatibility between the strain in the unbonded prestressing FRP tendon and the concrete at every cross section in a member. The increment of stress in the tendon due to applied loading should be evaluated by considering deformation of the whole member, rather than at a section, as for a bonded member.

Many attempts have been made by investigators to estimate the stress in a tendon at different loading conditions, especially at the ultimate nominal flexural resistance for concrete members prestressed with unbonded steel tendons. The principal difference between unbonded steel and FRP tendons is the modulus of elasticity. Thus, models for unbonded steel tendons serve as a basis for developing guidelines for unbonded FRP tendons. A method based on determining the strain in the critical section (maximum moment) was proposed by Naaman (1987) for steel tendons and later extended to FRP tendons (Naaman et al. 2002). The method assumes compatibility of strains, as if the tendons were bonded, and applies a strain reduction factor Ω to account for the fact that the tendons were unbonded. The increment in strain at the critical section is as shown in Eq. (7-2).

$$\Delta \varepsilon_{average} = (\Delta \varepsilon_p)_{unbonded} = \Omega(\Delta \varepsilon_p)_{bonded} \qquad (7\text{-}2)$$

The strain $(\Delta \varepsilon_p)_{bonded}$ can be computed using strain compatibility and, assuming linear elastic behavior of the tendon, the change in stress Δf_p in the unbonded tendon is given by

$$\Delta f_p = \Omega_u E_p \varepsilon_{cu} \left(\frac{d_p}{c_u} - 1 \right) \qquad (7\text{-}3)$$

where ε_{cu} is the strain in the extreme compression fiber at ultimate, and c_u is the depth of the neutral axis at ultimate.

Equation (7-1) can then be written as

$$f_p = f_{pe} + \Omega_u E_p \varepsilon_{cu} \left(\frac{d_p}{c_u} - 1 \right) \qquad (7\text{-}4)$$

Combining Eq. (7-4) with the equilibrium equation for a flanged section results in

$$0.85 f_c' b_w \beta_1 c_u + 0.85 f_c' (b - b_w) h_f = \qquad (7\text{-}5)$$

$$A_p f_p + A_s f_y - A_s' f_y'$$

where A_s' = area of nonprestressed compressive reinforcement; A_s = area of nonprestressed tensile reinforcement; f_y = yield strength of nonprestressed tensile reinforcement; f_y' = yield strength of nonprestressed compressive reinforcement; b = width of compression flange; b_w = width of web; and h_f = thickness of compression flange, gives a quadratic equation in c_u having the following root

$$c_u = \frac{-B + \sqrt{(B^2 - 4AC)}}{2A} \qquad (7\text{-}6)$$

where

$A = 0.85 f_c' b_w \beta_1;$

$B = A_p(E_p \varepsilon_{cu} \Omega_u - f_{pe}) + A_s' f_y' - A_s f_y + 0.85 f_c'(b - b_w)h_f;$ and

$C = -A_p E_p \varepsilon_{cu} \Omega_u d_p$

The strain reduction coefficient at ultimate, Ω_u, depends on a number of variables, such as loading configuration and extent of the cracks in a beam and varies theoretically between 0 and 1.0, with a value of 1.0 corresponding to a bonded tendon. The following values for Ω_u at ultimate were suggested by Alkhairi (1991) based on a regression analysis on test data from 143 beams prestressed with steel tendons

$$\Omega_u = \frac{2.6}{(L/d_p)} \text{ (for one-point loading)} \qquad (7\text{-}7a)$$

$$\Omega_u = \frac{5.4}{(L/d_p)} \text{ (for two-point or uniform loading)} \qquad (7\text{-}7b)$$

For design purposes, Alkhairi (1991) recalibrated the coefficient Ω_u in such a way that most of the predicted values are smaller than the experimental results and made the following recommendations

$$\Omega_u = \frac{1.5}{(L/d_p)} \text{ (for one-point loading)} \qquad (7\text{-}7c)$$

$$\Omega_u = \frac{3.0}{(L/d_p)} \text{ (for two-point or uniform loading)} \qquad (7\text{-}7d)$$

Recent research at Queen's University (Gangkatharan 2003) has indicated that Eq. (7-7c) and (7-7d) are applicable to beams containing CFRP tendons having an unbonded length greater than 15 times the depth of the beam.

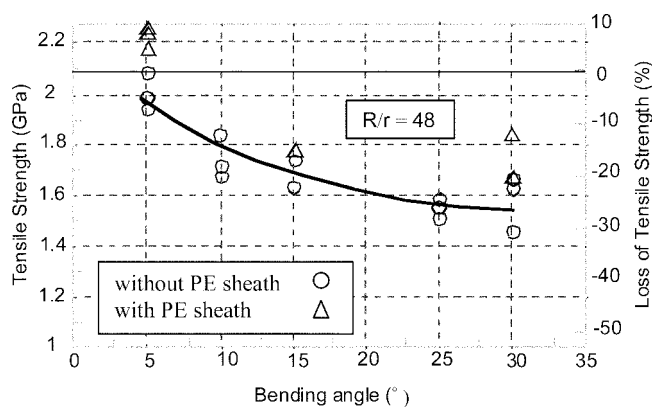*Fig. 7.1—Saddles used on the Bridge Street Bridge (Grace et al. 2002).*

Fig. 7.2—Relationship between the tensile strength with the angle of curvature and with the radius of curvature (after Santoh [1993]).

7.2—External prestressing

7.2.1 *General*—Externally prestressed systems consist of unbonded tendons located outside the beam cross-sectional area and post-tensioned against anchorages and deviators attached to or built into the beam. The tendons may be external to the cross section or may be in the void of a box section. External prestressing has the advantage of reducing the dead load of a structure due to the reduction in web thickness as a result of eliminating internal ducts, easing inspection of tendons and replacement of old or damaged tendons, and improving shear resistance due to the elimination of shear resistance deficiencies that are present at internal duct locations. Some of the practical difficulties of this system include providing anchorage for the post-tensioning tendons and maintaining the lateral stability of the girders during post-tensioning. In addition, the tendons are exposed and therefore are susceptible to damage during construction and throughout their service life. Suitable protection should be provided for the external tendons during the life of the structure.

Straight and harped tendon profiles can be used. For harped tendons, deviation saddles are used to hold the tendons in place and transfer components of the prestressing force from the tendons into the concrete girder.

7.2.2 *Internal versus external unbonded tendons*—One of the main differences between external and internal unbonded tendons is the variation of eccentricity in the case of external tendons during deformation of the beam under load. This variation is caused by the external tendon remaining rectilinear between the deviators and the end anchorages, while the beam deformation is curvilinear. Therefore, the eccentricity of an external prestressing tendon changes as the loading progressively increases to ultimate. Thus, it is necessary to investigate the deformation behavior of externally prestressed members throughout all stages of loading.

7.2.3 *Design considerations*—The effect of tendon bending at the deviator points on the ultimate strength of the cables should be taken into consideration when using FRP as externally prestressed draped tendons. Special saddles should be designed to avoid inducing stress concentrations in the tendon by providing a system with limited curvature, friction, and sufficient area to limit the lateral stresses on the tendon. Figure 7.1 shows the saddle used on the Bridge Street bridge (Grace et al. 2002). Figure 7.2, adopted from the Tokyo Rope catalog (Santoh 1993), depicts the relationship between the tensile strength of the CFCC and the angle of curvature through which the tendon is bent. A reduction in the tendon strength is observed as the angle of curvature increases and is similar to the discussion in Section 3.9. This reduction in strength of the CFCC can be mitigated by flaring the strands at the harp points, and by reducing the friction between the CFCC tendons and the saddle by providing a cushioning material, such as low-density polyethylene (PE), on the saddle. This is particularly important when the angle of bend at the saddle is larger than 5 degrees. The effects of drape angle on the strength of Leadline™ and CFCC have been discussed by Grace and Abdel-Sayed (1998b).

External tendons are designed to ensure longitudinal prestressing of a beam and generally represent only a portion of the total flexural reinforcement. The remaining reinforcement may consist of internal prestressed reinforcement, nonprestressed reinforcement, or a combination of both, depending on the structural system and the type of construction. A minimum amount of bonded reinforcement is also necessary to control the distribution of cracks and to limit the crack widths.

7.2.4 *Stress at ultimate in external unbonded prestressed tendons*—Aravinthan and Mutsuyoshi (1997) investigated the stress in external unbonded prestressed steel tendons and noted that the variations in the eccentricity could have a significant influence on the ultimate strength of externally prestressed beams. As a result, they introduced the concept of depth reduction factor R_d to estimate the effective depth d_e of an external tendon at ultimate as follows

$$d_e = R_d d_p \qquad (7\text{-}8)$$

where

$$R_d = 1.14 - 0.005\left(\frac{L}{d_p}\right) - 0.19\left(\frac{S_d}{L}\right) \le 1.0 \qquad (7\text{-}9a)$$

for one-point loading; and

$$R_d = 1.25 - 0.010\left(\frac{L}{d_p}\right) - 0.38\left(\frac{S_d}{L}\right) \le 1.0 \qquad (7\text{-}9b)$$

for third-point loading;

and S_d is the spacing of the deviators, and L is the span of the beam.

Based on a parametric evaluation, Aravinthan and Mutsuyoshi (1997) proposed alternative equations for the strain reduction coefficient Ω_u. These equations, which they claim can be used to predict the behavior at ultimate of beams with external prestressing or a combination of internal and external prestressing, are as follows

$$\Omega_u = \frac{0.21}{(L/d_p)} + 0.04\left(\frac{A_{p\,int}}{A_{p\,tot}}\right) + 0.04 \qquad (7\text{-}10a)$$

for one-point loading; and

$$\Omega_u = \frac{2.31}{(L/d_p)} + 0.21\left(\frac{A_{p\,int}}{A_{p\,tot}}\right) + 0.06 \qquad (7\text{-}10b)$$

for third-point loading

where $A_{p\,int}$ is the area of the internal prestressed reinforcement, and $A_{p\,tot}$ is the total area of internal and external prestressed reinforcement.

The values of Ω_u from Eq. (7-10) can be incorporated in Eq. (7-4) with d_p replaced by d_e to determine the stress at ultimate.

The significance of change in the eccentricity of the external tendons during loading in the calculation of the stress at ultimate has been corroborated by Rao and Mathew (1996) and Tan and Ng (1997). The applicability of above equations to FRP prestressed tendons needs to be established.

CHAPTER 8—PILE DRIVING AND IN-PLACE FLEXURE

8.1—General

Piles are commonly installed by a succession of blows that are applied using a drop, diesel, steam, or compressed-air-powered hammer. Four types of damage may occur during driving of prestressed concrete piles:

- Concrete spalling at the pile head due to high compressive stresses;
- Concrete spalling at the pile tip due to hard driving resistance;
- Transverse cracking due to tensile stress reflected from the pile tip or pile head; and
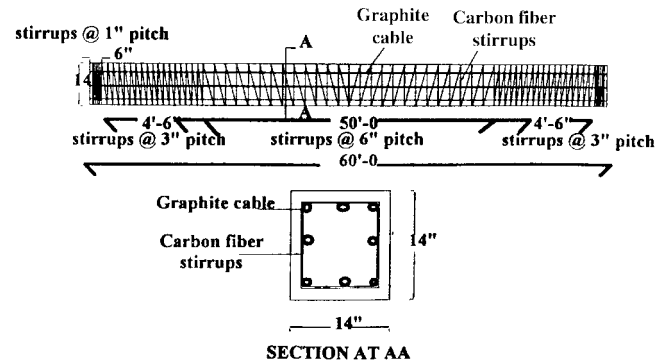- Spiral or transverse cracking due to combined torsion and tensile stress.

Fig. 8.1—Pile details (Iyer et al. 1996).

Though identified for steel prestressed piles, this type of damage may be anticipated in FRP prestressed piles as well. Although FRP prestressed piles may provide the same effective prestress, verification of their performance is required to allay concerns relating to the use of any new material. Specifically, the effectiveness of confinement provided by FRP ties needs to be proven. Additionally, it is necessary to demonstrate that there is no debonding of the FRP strands under impact loading and consequent loss of effective prestress.

8.2—Demonstration studies

Four studies have been conducted in the United States in which full-size FRP prestressed concrete piles were driven and monitored to verify their performance. In the earliest study by Sen, Issa, and Mariscal (1992) and Sen et al. (1993), S-2 glass strands were used for prestressing. In subsequent studies, CFRP material was tested by Iyer (1995), Iyer et al. (1996), Arockiasamy and Amer (1998), and Schiebel and Nanni (2000).

8.2.1 *Study by Iyer (1995) and Iyer et al. (1996)*—Twelve CFRP prestressed piles were used to support two 6.1 m (20 ft) bays of a composite pier at the Naval Facilities Engineering Service Center, Port Hueneme, Calif. The piles were 18.3 m (60 ft) long, 356 mm (14 in.) square, and prestressed by eight 12.5 mm (1/2 in.) CFRP strands with 9.5 mm (3/8 in.) CFRP spirals. The eight strands were stressed to provide an effective prestress of 4.83 MPa (700 psi). Figure 8.1 shows the layout and cross section of the piles.

A 17.8 kN (4000 lb) hammer was used to drive the piles. The subsurface below the mudline consisted of well-graded moderately dense silty sands with intermittent silty clay and clayey silt lenses. Figure 8.2 shows the installation of the CFRP piles.

The maximum measured compressive stresses ranged from 20.7 to 23.4 MPa (3 to 3.4 ksi) and were below the recommended limit of 30.3 MPa (4.4 ksi). The pile cushion employed a fresh stack of plywood with a predriving thickness of 125 mm (5 in.). A visible surface crack was noticed after 263 blows at a location 7.62 m (25 ft) from the pile top. The installation was temporarily stopped and continued after an additional 125 mm (5 in.) plywood cushion was placed on the pile top and the hammer reset to a lower level. Maximum computed pile tensile stress reached 6.41 MPa (0.93 ksi) before the adjustment. The pile was successfully installed

Fig. 8.2—View of installation of CFRP test pile (Iyer 1995).

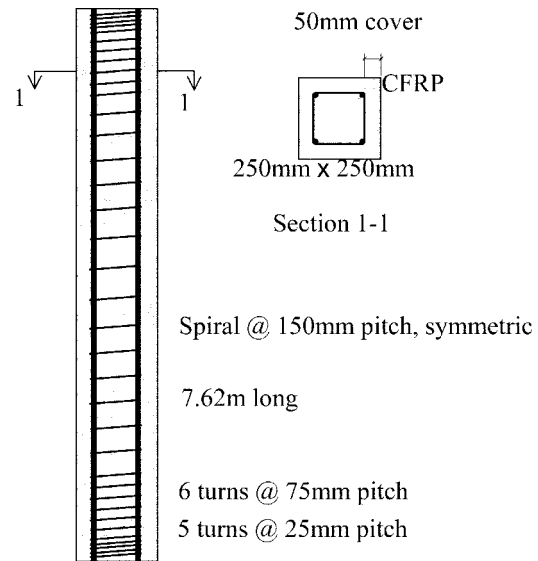Fig. 8.3—Construction on CFRP prestressed piles supporting pier.

Fig. 8.4—CFRP pile details (Arockiasamy and Amer 1998).

are shown in Fig. 8.4. The all-CFRP piles used CFCC 1 x 7 7.5 mm (0.3 in.) diameter strands as spiral ties. The spacing of the spirals was the same as that used by Iyer et al. (1996) (Fig. 8.1). Steel spirals having a diameter of 5 mm (0.2 in.) were used in the two other specimens. The ultimate strength of the CFRP spirals was 2117 MPa (307 ksi) versus 1034 MPa (150 ksi) for the steel spirals. Prestressing was provided by four CFCC 1 x 7 12.5 mm (0.5 in.) strands produced by Tokyo Rope. The jacking stress was designed to produce an average compressive stress of 5.5 MPa (800 psi). This effective stress was comparable to that recommended by ACI 543R. A 13.4 kN (3012 lbf) hammer was used to drive the piles.

The average specified drop height was 1.82 m (6 ft), though it averaged 2.12 m (7 ft) based on the energy transferred to the top of the piles. The stresses predicted by wave analysis varied between 0 to 7.1 MPa (0 to 1.03 ksi) tensile and 16.6 to 24.3 MPa (2.41 to 3.53 ksi) compressive strength and were in reasonable agreement with the experimental results. The tensile stresses were maximum at the initial stage of driving while the compressive stresses were higher at the end of the driving stage. All stresses were within the limits permitted by the Florida Department of Transportation (FDOT) specifications. No damage was observed in the piles.

8.2.3 *Study by Schiebel and Nanni (2000)*—Four 7.3 m (24 ft) long by 300 mm (12 in.) by 300 mm (12 in.) cross-sectional piles were fabricated. Two of these piles were CFRP prestressed and two others were prestressed using steel strands. CFRP spirals were used over a portion of the CFRP prestressed pile. Of the four piles, two—one CFRP prestressed and one steel prestressed pile—were driven. The other two were subject to flexural tests in the laboratory. CFRP spirals have a 3.62 GPa (525 ksi) guaranteed tensile strength. Two identical sections of spiral were fabricated, one for each of the two piles. Each spiral section had 21 turns (five turns at 25 mm [1 in.] pitch and 16 turns at 75 mm [3 in.] pitch for a total length of 1.325 m [53 in.] [Fig. 8.5]). The spiral sections were installed in the driven end of the piles.

with no propagation of the surface crack while tensile stresses remained below 5.9 MPa (0.85 ksi).

Although the piles were 18.3 m (60 ft) long, the required bearing capacity was reached after 13.7 m (45 ft). As a result, all piles were cut to 13.7 m (45 ft) and then driven on site. This meant that the spiral spacing was increased to 150 mm (6 in.) from the end one spacing of 25 mm (1 in.) (Fig. 8.1). There were no cracks in the shortened installed piles. A view of the construction and installation of the CFRP piles is shown in Fig. 8.3.

8.2.2 *Study by Arockiasamy and Amer (1998)*—In this study, four 7.62 m (25 ft) long by 250 mm (10 in.) square CFRP prestressed piles were fabricated and tested. Two of the piles used CFRP spirals while two others used steel spirals. Details of the cross section of the pile and tie spacing
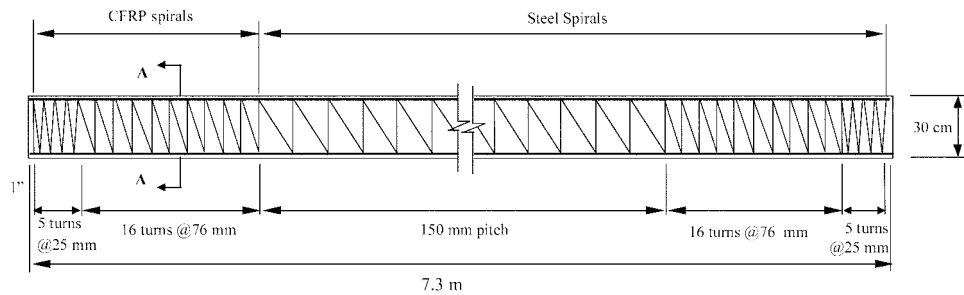
Fig. 8.5—Pile details (Schiebel and Nanni 2000).

The rest of the pile section was confined with conventional steel spirals.

A 14.4 kN (3240 lbf) hammer was used to drive the piles (Fig. 8.6). The piles were driven into a rocky-clay fill material on the approach to a new bridge. Neither pile was driven to bedrock. Once the pile was driven, the pile head was inspected for damage. Aside from some minor chipping at the square edges, no damage was observed. Static field-testing indicated that there was no reduction in flexural capacity.

8.3—Discussion

Piles are prestressed to withstand tensile stresses that arise when they are driven through soft soils. FRP and steel may be used to develop the same effective prestress. As FRP is stressed to a smaller fraction of its ultimate tensile strength and its interface with concrete differs from steel, transfer lengths will differ. Arockiasamy and Amer (1998) found that transfer length for the CFRP strands was 40 diameters (compared with 50 diameters for prestressed steel). For 12.5 mm (0.5 in.) strands, this amounts to 125 mm (5 in.) difference in the location where the full effective prestress is transferred to the pile. For this case, the performance of the CFRP would be marginally better.

8.4—Conclusions

The principal conclusions from the demonstration studies are:

1. The performance of FRP prestressed and steel prestressed piles during driving are similar;

2. The majority of the piles relied on friction rather than end-bearing for support;

3. FRP ties performed satisfactorily based on the absence of damage following the driving operation. The tie spacing used was identical to that in comparable steel prestressed piles;

4. The FRP prestressed piles that are properly engineered in terms of effective prestress and lateral ties provided, and employ driving parameters based on wave analysis, may be expected to perform satisfactorily; and

5. The results indicate that there are no inherent problems in driving FRP prestressed piles.

An assessment of the test reports suggest the following guidelines for FRP prestressed piles:

1. The specified strength of concrete should be at least 41.4 MPa (6000 psi) to prevent compression failure;

Fig. 8.6—View of installation of hybrid CFRP/steel (Schiebel and Nanni 2000).

2. The cover for steel prestressed piles is 75 mm (3 in.). Such large covers are not needed for corrosion-resistant FRP material. Recommendations in specifications for FRP reinforcement may be used;

3. Effective prestress should be between 4.8 to 5.5 MPa (700 to 800 psi);

4. FRP spiral ties provided should have twice the ultimate capacity as steel ties. The same spacing used in steel prestressed piles should be used for FRP prestressed piles;

5. FRP prestressed piles should be installed following the recommendations in ACI 543R;

6. Driving stresses in selected FRP test piles need to be carefully monitored using a pile dynamic analyzer (PDA); and

7. A predriving analysis is required for selection of the pile hammer, the drop height, and the thickness of the pile and helmet cushions to ensure driving stresses comply with limits set in project specifications.

CHAPTER 9—RESEARCH NEEDS

While there is a substantial volume of laboratory tests and field installations, a number of research areas remain to be investigated. The following represent the committee's major concerns.

Tendon and anchorage systems—The lack of commercial tendon and anchorage systems remains a major impediment to the industry. Without a commercial system, every project

remains a research endeavor. This concern extends to the economics of FRP tendons. The current price premium makes them uneconomical for many applications.

Anchorages—Anchorages need additional development in several areas. Field and construction-friendly anchorages are needed. The fatigue effects at anchorages for unbonded systems need evaluation.

Fire protection—Even though carbon fibers may be heat resistant to 1000 °C (1800 °F), the resins are generally sensitive to heat. Fire protection of anchorages is also of concern.

Harping devices—The larger radii needed to limit stresses make commercial push-down and roller-harping devices unsuitable. New harping devices and saddles need to be developed.

Long-term bond—The FRP tendon bond depends on the resin surface. While there is some experience with epoxy-coated steel bars, the long-term durability behavior of bond in FRP prestressing tendons is not yet defined.

Galvanic action—Carbon fibers are higher on the galvanic table than steel, creating a potential corrosion problem. The resin bonding agents may preclude this effect, but research is needed to investigate this behavior and provide design guidance.

External post-tensioning for rehabilitation—FRP has potential for rehabilitation applications. The lower elastic modulus of FRP makes stressing short tendons more attractive. The lack of tendon-anchorage systems remains a key application issue.

Tendon replacement—FRP replacement tendons for corroded structures are an application area with high potential. The design of a tendon to fit in the existing duct and to function over tendon bend points in the reinforcement needs to be resolved.

Circular prestressed tanks—Design guides for prestressing circular "wire- and strand-wrapped" tanks using FRP tendons need to be developed.

Stressing procedure—Guidelines for stressing procedure/ methods need to be developed.

Reliability assessment—The strength-reduction factors require recalibration to ensure conformance with the load factors in ACI 318-02.

Shear capacity—Shear design guidelines for FRP prestressed beams with FRP stirrups need further development.

Bond and development—Protocols for validation of FRP tendon transfer length and development length are needed.

CHAPTER 10—REFERENCES
10.1—Referenced standards and reports

The standards and reports listed below were the latest editions at the time this document was prepared. Because these documents are revised frequently, the reader is advised to contact the proper sponsoring group if it is desired to refer to the latest version.

American Concrete Institute

ACI 116R   Cement and Concrete Notation

ACI 440R   State-of-the-Art Report on Fiber Reinforced Plastic (FRP) Reinforcement for Concrete Structures

ACI 440.1R   Guide for the Design and Construction of Concrete Reinforced with FRP Bars

ACI 543R   Design, Manufacture, and Installation of Concrete Piles

AASHTO

AASHTO   Standard Specifications for Highway Bridges

Canadian Standards Association

CAN/CSA S6   Canadian Highway Bridge Design Code

CAN/CSA S806   Design and Construction of Building Components with Reinforced Polymers

These publications may be obtained from these organizations:

American Concrete Institute
P.O. Box 9094
Farmington Hills, MI 48333-9094

AASHTO
444 North Capitol St. N.W., Suite 249
Washington, DC 20001

Canadian Standards Association
178 Rexdale Blvd.
Toronto, ON
M9W 1R3 Canada

10.2—Cited references

Abdelrahman, A. A., and Rizkalla, S. H., 1998, "Deflection Control of Concrete Beams Pretensioned by CFRP Reinforcements," *Journal of Composites for Construction*, ASCE, Feb., pp. 55-62.

Abdelrahman, A. A.; Tadros, G.; and Rizkalla, S. H., 1995, "Test Model for the First Canadian Smart Highway Bridge," *ACI Structural Journal*, V. 92, No. 4, July-Aug., pp. 451-458.

ACI Committee 318, 2002, "Building Code Requirements for Structural Concrete (ACI 318-02) and Commentary (318R-02)," American Concrete Institute, Farmington Hills, Mich., 443 pp.

Alkhairi, F. M., 1991, "On the Behavior of Concrete Beams Prestressed with Unbonded Internal and External Tendons," PhD thesis, University of Michigan, Ann Arbor, Mich., 415 pp.

Al-Mayah, A.; Soudki, K. A.; and Plumtree, A., 2001, "Experimental and Analytical Investigation of a Stainless Steel Anchorage for CFRP Pretensioning Tendons," *PCI Journal*, V. 46, No. 2, pp. 88-100.

Aravinthan, T., and Mutsuyoshi, H., 1997, "Prediction of the Ultimate Flexural Strength of Externally Prestressed PC Beams," *Transaction of the Japan Concrete Institute*, V. 19, pp. 225-230.

Arockiasamy, M., and Amer, A., 1998, "Studies on CFRP Prestressed Concrete Bridge Columns and Piles in Marine Environment," Final Report Submitted to Florida Department of Transportation, Tallahassee, Fla., July.

Bakis, C. E., 1993, "FRP Composites: Materials and Manufacturing," *Fiber-Reinforced-Plastic for Concrete Structures*, A. Nanni, ed., Elsevier, Amsterdam, Chapter 3, pp. 13-58.

Bakis, C. E.; Bhat, B. B.; Schokker, A. J.; and Boothby, T. E., 2001, "Flexure of Concrete Beams Prestressed with FRP Tendons," *Proceedings of the Fifth International Symposium on Fiber Reinforced Polymer Reinforcement for Concrete Structures (FRPRCS-5),* Cambridge, London, pp. 689-697.

Braimah, A.; Green, M. F.; and Soudki, K. A., 1996, "Eliminating Steel from Bridge Deck Slabs by Combining CFRP Tendons with Polypropylene FRC," *Proceedings of the Second International Conference on Advanced Composite Materials in Bridges and Structures (ACMBS2)*, Montreal, Quebec, Canada, Aug., pp. 735-742.

Bryan, P. E., and Green, M. F., 1996, "Low Temperature Behavior of CFRP Prestressed Concrete Beams," *Canadian Journal of Civil Engineering*, V. 23, No. 2, pp. 464-470.

Burgoyne, C. J., 1988, "Engineering Applications of Parafil Rope," *Symposium on Engineering Applications of Parafil Rope*, Imperial College, London, pp. 39-47.

Burke, B.; Nelson, J.; and Dolan, C. W., 2000, "Friction Loss of CFRP Post-Tensioned Tendons," *Proceedings of the Third International Conference on Advanced Composite Materials in Bridges and Structures (ACMBS3)*, Ottawa, Canada, Aug., pp. 249-257.

Campbell, T. I.; Shrive, N. G.; Soudki, K. A.; Al-Mayah, A.; Keatley, J. P.; and Reda, M. M., 2000, "Design and Evaluation of a Wedge-Type Anchor for Fiber Reinforced Polymer Tendons," *Canadian Journal of Civil Engineering*, V. 27, pp. 985-992.

Currier, J., 1995, "Deformation of Prestressed Concrete Beams with FRP Tendons," MS thesis, Department of Civil and Architectural Engineering, University of Wyoming, Laramie, Wy., 112 pp.

Dolan, C. W., 1989, "Prestressed Concrete Using KEVLAR Reinforced Tendons," PhD dissertation, Cornell University, Ithaca, N.Y., 204 pp.

Dolan, C. W., 1990, "Developments in Non-Metallic Prestressing Tendons," *PCI Journal*, V. 35, No. 5, Sept., p. 80.

Dolan, C. W., 1999, "FRP Prestressing in the USA," *Concrete International*, V.21, No. 10, Oct., pp. 21-24.

Dolan, C. W., and Burke, C. R., 1996, "Flexural Strength and Design of FRP Prestressed Beams," *Proceedings of the Second International Conference on Advanced Composite Materials in Bridges and Structures (ACMBS2)*, Montreal, Quebec, Canada, Aug., pp. 383-390.

Dolan, C. W.; Hamilton, H. R.; Bakis, C. E.; and Nanni, A., 2000, "Design Recommendations for Concrete Structures Prestressed with FRP Tendons, Final Report," *Department of Civil and Architectural Engineering Report DTFH61-96-C-00019*, University of Wyoming, Laramie, Wyo., May, 113 pp.

Dolan, C. W., and Swanson, D., 2002, "Development of Flexural Capacity of FRP Prestressed Beam with Vertically Distributed Tendons," *Composites Part B: Engineering*, V. 3, No. 1, Elsevier, New York, 2002, pp. 1-6.

Domenico, N., 1995, "Bond Properties of CFCC Prestressing Strands in Pretensioned Concrete Beams," MSc thesis, Department of Civil Engineering, University of Manitoba, Winnipeg, Manitoba, Canada, 160 pp.

Dowden, D. M., and Dolan, C. W., 1997, "Comparison of Experimental Shear Data for FRP Prestressed Beams with Code Provisions" *Proceedings*, FRPRCS-3, V. 2, Sapporo, Japan, Oct., 687 pp.

Dye, W. K.; Bakis, C. E.; and Nanni, A., 1998, "Accelerated Testing of Carbon FRP Tendon-Anchor Systems for Post-Stressed Concrete Applications," *Proceedings of the First International Conference on Durability of Composites for Construction*, V. 2, Sherbrooke, Quebec, Canada, pp. 463-473.

Ehsani, M. R.; Saadatmanesh, H.; and Nelson, C. T., 1997, "Transfer and Flexural Bond Performance of Aramid and Carbon FRP Tendons," *PCI Journal*, V. 42, No. 1, Jan.-Feb., pp. 76-86.

Ehsani, M. R.; Saadatmanesh, H.; and Tao, S.; 1995, "Bond of Hooked Glass Fiber Reinforced Plastic (GFRP) Reinforcing Bars to Concrete," *ACI Materials Journal*, V. 92, No. 4, July-Aug., pp. 391-400.

Fam, A. Z.; Rizkalla, S. H.; and Tadros, G., 1997, "Behavior of CFRP for Prestressing and Shear Reinforcements of Concrete Highway Bridges," *ACI Structural Journal*, V 94, No. 1, Jan.-Feb., pp. 77-86.

FIB TG9.3, http://allserv.rug.ac.be/~smatthys/fibTG9.3/

FIP, 1992, "High-Strength Fiber Composite Tensile Elements for Structural Concrete," *FIP Commission on Prestressing Materials and Systems*, Institute of Structural Engineers, London, July, 160 pp.

Fukuyama, H., 1999, "FRP Composites in Japan," *Concrete International*, V. 21, No. 10, Oct., pp. 29-32.

Gangkatharan, J., 2003, "Strength of Partially Unbonded Prestressed Concrete Beams," MSc thesis, Queen's University, Kingston, Canada, 134 pp.

Gerritse A., and Werner, J., 1988, *ARAPREE: The Prestressing Element Composed of Resin Bonded Twaron Fibers*, Holland Beton Group, The Netherlands, June, 8 pp.

Gerritse, A. and Werner, J., 1991, "ARAPREE—A Non-Metallic Tendon," *Advanced Composite Materials in Civil Engineering Structures*, ASCE, Materials Engineering Division, New York, pp. 143-154.

Grace, N. F., 1999, "Continuous CFRP Prestressed Concrete Bridges," *Concrete International,* V. 21, No. 10, Oct., pp. 42-47.

Grace, N. F., 2000a, "Transfer Length of CFRP/CFCC Strands for Double-T Girders," *PCI Journal*, V. 45, No. 5, Sept.-Oct. 2000, pp. 110-126.

Grace, N. F., 2000b, "Response of Continuous CFRP Prestressed Concrete Bridges Under Static and Repeated Loadings," *PCI Journal*, V. 45, No. 6, Nov.-Dec., pp. 84-101.

Grace, N. F., and Abdel-Sayed, G., 1998a, "Ductility of Prestressed Bridges using CFRP Strands," *Concrete International*, V. 20, No. 6, June, pp. 25-30.

Grace, N. F., and Abdel-Sayed, G., 1998b, "Behavior of Externally Draped CFRP Tendons in Prestressed Concrete Bridges," *PCI Journal*, V. 43, No. 5. Sept.-Oct., pp. 88-101.

Grace, N. F.; Enomoto, T.; and Yagi, K., 2002, "Behavior of CFCC and CFRP Leadline Prestressing Systems in Bridge Construction," *PCI Journal*, V. 47, No. 3, May-June, pp. 90-103.

Grace, N. F.; Navarre, F. C.; Nacey, R. B.; Bonus, W.; and Collavino, L., 2002, "Design-Construction of Bridge Street Bridge—First CFRP Bridge in the United States," *PCI Journal*, V. 47, No. 5. Sept.-Oct., pp. 20-35.

Grace, N. F., and Singh, S. B., 2003, "Design Approach for Carbon Fiber-Reinforced Polymer Prestressed Concrete Bridge Beams," *ACI Structural Journal*, V. 100, No. 3, May-June, pp. 365-376.

Harada, T.; Idemitsu, T.; Watanabe, A.; Khin, M.; and Soecha, K., 1993, "New FRP Tendon Anchorage System Using Highly Expansive Material for Anchoring," *FIP Symposium 93*, Kyoto, pp. 711-718.

Harada, T.; Soeda, M.; Enomoto, T.; Tokumitsu, S.; Khin, M.; and Idemitsu, T., 1997, "Behavior of Anchorage for FRP Tendons Using Highly Expansive Material Under Cyclic Loading," *Non-Metallic Reinforcement for Concrete Structures*, Sapporo, Proceedings FRPRCS-3, V. II, pp. 719-726.

Hartman, D. R.; Greenwood, M. E.; and Miller, D. M., 1994, "High Strength Glass Fibers," *Technical Paper 1-PL-19025*, Owens Corning Fiberglas Corp., Toledo, Ohio, Mar.

Holte, L. E.; Dolan, C. W.; and Schmidt, R. J., 1993, "Epoxy Socketed Anchors for Non-Metallic Prestressed Tendons," *Fiber-Reinforced-Plastic Reinforcement of Concrete Structures*, SP-138, A. Nanni and C. W. Dolan, eds., American Concrete Institute, Farmington Hills, Mich., pp. 381-400.

IABSE, 2003, "Use of Fiber Reinforced Polymers in Bridge Construction," *Structural Engineering Documents* No. 7, IABSE-AIPC-IVBH, Zurich, Switzerland.

Iyer, S. L., 1993, "First Composite Cable Prestressed Bridge in the USA," *Proceedings of the Thirty-Eight International SAMPE Symposium*, Anaheim, Calif.

Iyer, S. L., 1995, "Demonstration of Advanced Composite Cables for use as Prestressing in Concrete Waterfront Structures," Final report submitted to U.S. Army Corps of Engineers, Construction Engineering Research Laboratory, Champaign, Ill., Nov.

Iyer, S. L., and Kumarswamy, C., 1988, "Performance Evaluation of Glass Fiber Composite Cable for Prestressing Concrete Units," *Proceedings of the Thirty Third International SAMPE Symposium*, Anaheim, Calif, Mar.

Iyer, S.; Lampo, R.; Hoy, D.; and McCarthy, N., 1996, "First Navy Pier Built in the USA Using FRP Cables for Prestressing," *Proceedings of the International Conference on FRP in Civil Engineering at IIT Madras*, Dec., pp. 490-498.

Iyer, S. L., and Sen, R., 1991, "Advanced Composite Materials in Civil Engineering Structures," *Proceedings of Specialty Conference*, ASCE, Las Vegas, Nev.

Joint ACI-ASCE Committee 426, 1973, "The Shear Strength of Reinforced Concrete Members," *Proceedings*, ASCE, V. 99, No. ST6, pp. 1091-1187.

JSCE, 1992, "Application of Continuous Fiber Reinforcing Materials to Concrete Structures," *Concrete Library International*, No. 19, Japan Society of Civil Engineers, Tokyo, p. 89.

JSCE, 1993, "State-of-the Art Report on Continuous Fiber Reinforcing Materials," *Research Committee on Continuous Fiber Reinforcing Material*, A. Machida, ed., *Concrete Engineering Series* No. 3, Japan Society of Civil Engineers, Tokyo, Oct., 164 pp.

JSCE, 1996, "Research Committee on Continuous Fiber Reinforcing Materials: Recommendation for Design and Construction of Concrete Structures Using Continuous Fiber Reinforcing Materials," *Concrete Library* No. 88, Japan Society of Civil Engineers, Tokyo, Japan, Sept.

JSCE, 1997, "Recommendation for Design and Construction of Concrete Structures Using Continuous Fiber Reinforcing Materials," *Concrete Engineering Series* No. 23, 325 pp.

Kelly, D. J.; Bradberry, T. E.; and Breen, J. E., 1987, "Time-Dependent Deflections of Pretensioned Beams," *Research Report* 381-1, Research Project 3-5-84-381, Center for Transportation Research, Bureau of Engineering Research, University of Texas at Austin, Austin, Tex.

Kevlar Technical Guide, 1992, "Du Pont Fibers," Wilmington, Del., Dec., 134 pp.

Kim, P., and Meier, U., 1991, "CFRP Cables for Large Structures," *Proceedings of the Specialty Conference on Advanced Composites Materials in Civil Engineering Structures*, ASCE, Las Vegas, Nev., pp. 233-244.

Lu, Z.; Boothby, T. E.; Bakis, C. E.; and Nanni, A., 2000, "Transfer and Development Length of FRP Prestressing Tendons," *PCI Journal*, V. 45, No. 2, pp. 84-95.

Mahmoud, Z. I., and Rizkalla, S. H., 1996, "Bond of CFRP Prestressing Reinforcement," *Proceedings of the Second International Conference on Advanced Composite Materials in Bridges and Structures (ACMBS2)*, Montreal, Quebec, Canada, Aug., pp. 877-884.

Mahmoud, Z. I.; Rizkalla, S. H.; and Zaghloul, E., 1997, "Transfer and Development Length of CFRP Reinforcement," *Proceedings of the 1997 CSCE Annual Conference*, Sherbrooke, Quebec, May, pp. 101-110.

Malvar, L. J., and Bish, J., 1995, "Grip Effects in Tensile Testing of FRP Bars," *Proceedings of the Second International RILEM Symposium (FRPRCS-2)*, Non-Metallic (FRP) Reinforcement for Concrete Structures, Ghent, Belgium, Aug., pp. 108-115.

Mather, B., and Tye, R. V., 1955, "Plastic-Glass Fiber Reinforcement for Reinforced and Prestressed Concrete: Summary of Information Available as of July 1, 1955," *Technical Memorandum* No. 6-421, Report 1, Corps of Engineers, Waterways Experiment Station, Vicksburg, Miss.

Matthys, S., and Taerwe, L., 2001, "FRP Reinforcement: Developments in Europe," *Concrete International* V. 25, No. 6, June, pp. 20-21.

McKay, K. S., and Erki, M. A., 1993, "Flexural Behavior of Concrete Beams Pretensioned with Aramid Fiber Reinforced Plastic Tendons," *Canadian Journal Civil Engineering*, V. 20. No. 4, pp. 688-695.

MDA, 2004, Market Development Alliance of the FRP Composites Industry, www.mdacomposites.org/bridge_statistics.htm.

Mitsubishi Kasei Corp., 1993, "Leadline Carbon Fiber Tendons/Bars," *Product Specification Manual*, June, 18 pp.

Mufti, A. A.; Newhook, J. P.; and Tadros, G., 1996, "Deformability Versus Ductility in Concrete Beams with FRP Reinforcement," *Proceedings of the Second International Conference on Advanced Composite Materials in Bridges and Structures (ACMBS2),* Montreal, Quebec, Canada, Aug., pp. 189-199.

Naaman, A. E., 1987, "Partial Prestressing in the Rehabilitation of Concrete Bridges," *Proceedings of U.S.-European Workshop on Bridge Evaluation, Repair and Rehabilitation, St. Rémy-lès-Chevreux*, University of Michigan, Ann Arbor, Mich., June, pp. 392-406.

Naaman, A. E.; Burns, N.; French, C.; Gamble, W. L.; and Mattock, A. H., 2002, "Stresses in Unbonded Prestressing Tendons at Ultimate: Recommendation," *ACI Structural Journal*, V. 99, No. 4, July-Aug., pp. 520-531.

Naaman, A. E., and Jeong, S. M., 1995, "Structural Ductility of Concrete Beams Prestressed with FRP Tendons," *Non-metallic (FRP) Reinforcement for Concrete Structures*, Proceedings of the Second International RILEM Symposium (FRPRCS-2), Non-Metallic (FRP) Reinforcement for Concrete Structures, Ghent, Belgium, Aug., pp. 379-386.

Nanni, A.; Bakis, C. E.; O'Neil, E. F.; and Dixon, T. O., 1996a, "Performance of FRP Tendon-Anchor Systems for Prestressed Concrete Structures," *PCI Journal*, V. 41, pp. 34-44.

Nanni, A.; Bakis, C. E.; O'Neil, E. F.; and Dixon, T. O., 1996b, "Short-Term Sustained Loading of FRP Tendon-Anchor Systems," *Construction and Building Materials*, V. 10, pp. 255-266.

Nanni, A., and Dolan, C. W., eds., 1993, *Fiber-Reinforced-Plastic Reinforcement of Concrete Structures*, SP-138, American Concrete Institute, Farmington Hills, Mich., 977 pp.

Nanni, A., and Tanigaki, M., 1992, "Pretensioned Prestressed Concrete Members with Bonded Fiber Reinforced Plastic Tendons: Development and Flexural Bond Length (Static)," *ACI Structural Journal*, V. 89, No. 4, July-Aug., pp. 433-441.

Nanni, A.; Utsunomiya, T.; Yonekura, H.; and Tanigaki, M., 1992, "Transmission of Prestressing Force to Concrete by Bonded Fiber Reinforced Plastic Tendons," *ACI Structural Journal*, V. 89, No. 3, May-June, pp. 335-344.

NBS, 1976, "Non-Metallic Antenna Support Materials Pultruded Rods for Antenna Guys, Catenaries and Communications Structures," *Technical Report AFML-TR-76-42*, National Bureau of Standards, Washington, D.C., 126 pp.

Noritake, K.; Kakihara, R.; Kumagai, S.; and Mizutani, J., 1993, "Technora, an Aramid FRP Rod," *FRP Reinforcement for Concrete Structure: Properties and Applications*, A. Nanni, ed., Developments in Civil Engineering, V. 42. Elsevier Science Publishers B.V., Amsterdam. pp. 267-290.

PCI, 1975, "Recommendations for Estimating Prestress Losses," *PCI Journal*, V. 20, No. 4, July-Aug., pp. 43-75.

PCI, 2000, *Design Handbook*, Fifth Edition, Precast/Prestressed Concrete Institute, Chicago, Ill., 690 pp.

Pepper, L., and Mather, B., 1959, "Plastic-Glass Fiber Reinforcement for Reinforced Prestressed Concrete: Summary of Information from 1 July 1955 to 1 January 1959," *Technical Memorandum* No. 6-421 Report 2, Corps of Engineers, Waterways Experiment Station, Vicksburg, Miss.

Rao, S., and Mathew, G., 1996, "Behavior of Externally Prestressed Concrete Beams with Multiple Deviators," *ACI Structural Journal*, V. 93, No. 4, July-Aug., pp. 387-396.

Reda Taha, M. M., and Shrive, N. C., 2003a, "New Concrete Anchors for Carbon Fiber-Reinforced Post-Tensioned Tendons—Part 1: State-of-the-Art Review/Design," *ACI Structural Journal*, V. 100, No. 1, Jan.-Feb., pp. 86-95.

Reda Taha, M. M., and Shrive, N. C., 2003b, "New Concrete Anchors for Carbon Reinforced-Reinforced Post-Tensioned Tendons—Part 2: Development/Experimental Investigation," *ACI Structural Journal*, V. 100, No. 1, Jan.-Feb., pp. 96-104.

Rizkalla, N. S.; Fang, Z.; and Campbell, T. I., 2001, "Partially Bonded Partially Prestressed Pretensioned Beams with Hybrid FRP/Stainless Steel Reinforcement," *Proceedings of the Fifth International Symposium on Fiber Reinforced Polymer Reinforcement for Concrete Structures*, (FRPRCS-5), London, pp. 731-740.

Rizkalla, S. H., and Tadros, G., 1994, "A Smart Highway Bridge in Canada," *Concrete International*, V. 16, No. 6, June, pp. 42-44.

Salib, S. R.; Abdel-Sayed, G.; and Grace, N. F., 1999, "Crack Formation in Fiber Reinforced Polymers Concrete Beams," *Fiber Reinforced Polymer Reinforcement of Reinforced Concrete Structures: Selected Presentation Proceedings*, C. W. Dolan, S. H. Rizkalla, and A. Nanni, eds., American Concrete Institute, Farmington Hills, Mich., pp. 219-231.

Santoh, N., 1993, "CFCC: Carbon Fiber Composite Cable," *Fiber-Reinforced-Plastic (FRP) Reinforcement for Concrete Structures: Properties and Applications*, A. Nanni, ed., Developments in Civil Engineering, V. 42, Elsevier Science Publishers B.V., Amsterdam, pp. 223-248.

Sayed-Ahmed, E. Y., and Shrive, N. G., 1998, "A New Steel Anchorage System for Post-Tensioning Applications using Carbon Fiber Reinforced Plastic Tendons," *Canadian Journal of Civil Engineering*, V. 25, No. 1, pp. 113-127.

Schiebel, S., and Nanni, A., 2000, "Axial and Flexural Performance of Concrete Piles Prestressed with CFRP Tendons," *Proceedings of the Third International Conference on Advanced Composite Materials in Bridges and Structures (ACMBS3)*, Ottawa, Canada, Aug., pp. 471-478.

Sen, R.; Issa, M.; and Mariscal, D., 1992, "Feasibility of Fiberglass Pretensioned Piles in a Marine Environment," *Final Report No. CEM/ST/92/1* submitted to Florida Department of Transportation.

Sen, R.; Issa, M.; Wadsack, P.; and Shahawy, M., 1993, "Driving Stresses in Fiberglass Pretensioned Piles," *ACI Structural Journal*, V. 90, No. 6, Nov.-Dec., pp. 666-674.

Shaheen, E., 2004, "Carbon Fiber Reinforced Reactive Powder Concrete Anchorage System," PhD thesis, University of Calgary, Calgary, Alberta, Canada.

Shehata, E., 1999, "Fiber-Reinforced Polymer (FRP) for Shear Reinforcement in Concrete Structures," PhD thesis, Department of Civil and Environmental Engineering, University of Manitoba, Winnipeg, Canada.

Shield, C.; French, C.; and Hanus, J., 1999, "Bond of GFRP Rebar for Consideration in Bridge Decks," *Fiber Reinforced Polymer Reinforcement of Reinforced Concrete Structures*, SP-188, C. W. Dolan, S. H. Rizkalla, and A. Nanni, eds., American Concrete Institute, Farmington Hills, Mich., pp. 393-406.

Sonobe, Y.; Fukuyama, H.; Okamoto, T.; Kani, N.; Kimura, K.; Kobayashi, K.; Masuda, Y.; Matsuzaki, Y.; Mochizuki, S.; Nagasaka, T.; Shimizu, A.; Tanano, H.; Tanigaki, M.; and Teshigawara, M., 1997, "Design Guidelines of FRP Reinforced Concrete Building Structures," *Journal of Composite for Construction*, ASCE, V. 1, No. 3, pp. 90-115.

Soudki, K. A.; Green, M. F.; and Clapp, F. D., 1997, "Transfer Length of Carbon Fiber Rods in Precast Pretensioned Concrete Beams," *PCI Journal*, V. 42, No. 5, pp. 78-87.

Taerwe, L., and Matthys, S., 1999, "FRP for Concrete Construction: Activities in Europe," *Concrete International*, V. 21, No. 10, Oct., pp. 33-36.

Taerwe, L., and Pallemans, I., 1995, "Force Transfer of AFRP Bars in Concrete Prisms," *Proceedings of the Second International RILEM Symposium (FRPRCS-2),* Non-Metallic (FRP) Reinforcement for Concrete Structures, Ghent, Belgium, Aug., 154-163.

Tamura, T.; Kanda, M.; and Tsuji, Y., 1993, "Applications of FRP Materials to Prestressed Concrete Bridges and Other Structures in Japan," *PCI Journal*, V. 38, No. 4, pp. 50-58.

Tan, K. H., and Ng, C. K., 1997, "Effects of Deviators and Tendon Configuration on Behavior of Externally Prestressed Beams," *ACI Structural Journal*, V. 94, No. 1, Jan.-Feb., pp. 13-22.

Thornel, Continuous Pitch-Based Carbon Fibers Literature, 2004, www.cytec.com, Mar.

Torayca Technical Reference Manual, 1996, Toray Industries, Inc., Carbon Fibers Dept., Tokyo, Japan, 1996.

Triantafillou, T. C., and Deskovic, N., 1991, "Innovative Prestressing with FRP Sheets: Mechanics of Short Term Behavior," *Journal of Engineering Mechanics*, V. 117, No. 7, pp. 1652-1672.

Vijay, P. V., and GangaRao, H. V. S., 2001, "Bending Behavior and Deformability of Glass Fiber-Reinforced Polymer Reinforced Concrete Members," *ACI Structural Journal*, V. 98, No. 6, Nov.-Dec., pp. 834-842.

Wines, J. C.; Dietz, R. J.; and Hawley, J. L., 1966, "Laboratory Investigation of Plastic-Glass Fiber Reinforcement for Reinforced and Prestressed Concrete," *Report 1 & 2*, U.S. Army Corps of Engineers, Waterways Experiment Station, Vicksburg, Miss.

Wolff, R., and Miesseler, H.-J., 1989, "New Materials for Prestressing and Monitoring Heavy Structures," *Concrete International*, V. 11, No. 9, Sept., pp. 86-89.

Zoch, P.; Kimura, H.; Iwasaki, T.; and Heym, M., 1991, *Carbon Fiber Composite Cables—A New Class of Prestressing Members,* Transportation Research Board, Washington, D.C., 19 pp.

Zhang, B., 2002, "Experimental and Theoretical Investigations on New Bond-Type Anchorage System for Post-Tensioning Applications with FRP Tendons," PhD thesis, University of Sherbrooke, Canada.

APPENDIX A—DESIGN EXAMPLE
Example 1—Pretensioned single T-beam

A simply supported T-beam is to be designed to carry two 15 kip (67 kN) concentrated loads spaced 6.78 ft (2.1 m) on center. A Rocky Mountain Prestress 12DT40 section, cut in half along the centerline, is to be used for the section. The beam is to be designed to carry its self-weight plus live load. Tendons are harped at midspan with an end eccentricity of zero.

Procedure	Calculation in inch-pound units	SI equivalents
Step 1—Define section properties		
A	333 in.^{2}	214,800 mm^2
I_g	51,020 in.^{4}	2.124×10^{10} mm^4
S_t	3516 in.^{3}	57.6×10^6 mm^3
S_b	2001 in.^{3}	32.8×10^6 mm^3
S_p	2378 in.^{3}	39.0×10^6 mm^3
y_t	14.51 in.	369 mm
y_b	25.49 in.	647 mm
w_g	370 lb/ft	5.40 kN/m
e (eccentricity = y_b – cover)	21.49 in.	546 mm
b_w	7.25 in.	184 mm
b	72 in.	1829 mm
h	40 in.	1016 mm
h_f	2 in.	51 mm
d	36 in.	914 mm
Step 2—Define material properties		
f_c'	6500 psi	44.8 MPa
f_{ci}'	4000 psi	27.6 MPa
E_{ci}	3.08×10^6 psi	21.2 GPa
E_c	4.60×10^6 psi	31.7 GPa
$f_{ci} = 0.6f_{ci}'$	2400 psi	16.5 MPa
$f_{ti} = 3\sqrt{f_{ci}'}$	190 psi	1.3 MPa
$f_c = 0.45f_c'$	2925 psi	20.2 MPa
$f_t = 6\sqrt{f_c'}$	484 psi	3.3 MPa
Number of tendons – $m = 6$		
f_{pu}	425,000 psi	2.93 GPa
d_p	0.375 in.	9.5 mm
A_p	0.11 in.^{2}	71.0 mm^2
E_p	18,000 ksi	124 GPa
$\varepsilon_{cu} = f_{pu}/E_p$	425/18,000 = 0.024	0.024
Stress due to harping $= R_t E_p/R$	0.12(18,000)/24 = 90 ksi	620 MPa

Initial prestress = 60% f_{pu} less 20% for harping	Percent of strength = 100(90)/425 = 21.2%	
Stress tendon to 40% of f_{pu} to allow for harping $P_i = 0.40f_{pu}mA_p$	0.4(425)6(0.11) = 112.2 kips	499 kN
Step 3—Beam span and loadings		
Length L	39.37 ft	12.0 m
Load spacing b_1	6.78 ft	2.1 m
Shear span $a_1 = 1/2(L - b_1)$	1/2(39.37 – 6.78) = 13.16 ft	4.01 m
Dead load w	370 lbf/ft	5.40 kN/m
$M_d = wL^2/8$	0.370(39.37)2/8 = 71.7 ft-kips	97.2 kN-m
Live load P	15 kips	66.7 kN
$M_1 = Pa_1$	15 × 13.16 = 197 ft-kips	267 kN-m
$M_u = 1.2M_d + 1.6M_1$ (ACI 318-02)	1.2 × 71.7 + 1.6 × 197 = 401 ft-kips	544 kN-m
$V_u = 1.2wL/2 + 1.6P$	1.2 × 0.370 × 39.37/2 + 1.6 × 15 = 32.7 kips	145 kN
Step 4—Loss Calculations		
Modular ratio $n = E_f/E_{ci}$	n = 18,000/3080 = 5.8	
Elastic shortening $\Delta f_{es} = nf_{cp} = n(P_i/A + P_ie/S_p - M_d/S_p)$	5.8(112.2/333 + 112.2 × 21.45/2387 – 71.7 × 12/2387) = 5710 psi	39.4 MPa
Creep: assume 2 times initial elastic shortening $\Delta f_{cr} = C_c\Delta f_{es}$	2.0(5710) = 11,420 psi	78.7 MPa
Shrinkage: assume 0.0006 net strain at time of testing $\Delta f_s = \varepsilon_s E_p$	(0.0006)18,000,000 = 10,800 psi	74.5 MPa
Relaxation $\Delta f_r = 0.03f_{pi}$	0.03(0.4)425,000 = 5100 psi	35.2 MPa
Total losses $\Delta f_{es} + \Delta f_c + \Delta f_s + \Delta f_r$	5710 + 11,420 + 10,800 + 5100 = 33,030 psi	228 MPa
Total losses =	19.4%	19.4%
$f_{pe} = 0.4f_{pu}$ – losses	0.4(425) – 33.0 = 137.0 ksi	944 MPa
Final prestress = mA_pf_{pe}	6(0.11)137.0 = 90.4 kips	402 kN
Step 5—Check service level stresses at midspan		
Initial stresses		
Top = $P_i/A - P_ie/S_t + M_d/S_t$	112.2/333 – 112.2 × 21.45/3516 + 71.7 × 12/3516 = –0.108 ksi	–0.74 MPa
Bottom = $P_i/A + P_ie/S_b - M_d/S_b$	112.2/333 + 112.2 × 21.45/2001 – 71.7 × 12/2001 = 1.110 ksi	7.6 MPa
Both are within stress limits.		
Final stresses		
Top = $P_e/A - P_ee/S_t + M_d/S_t + M_1/S_t$	90.4/333 – 90.4 × 21.45/3516 + 71.7 × 12/3516 + 197 × 12/3516 = 0.635 ksi tension	4.38 MPa
Bottom = $P_e/A + P_ee/S_b - M_d/S_b - M_1/S_b$	90.4/333 + 90.4 × 21.45/2001 – 71.7 × 12/2001 – 197 × 12/2001 = 0.370 ksi tension	2.55 MPa
Both are within stress limits.		
Step 6—Check strength capacity		
Effective flange width $b_{eff} = L/4$	= 39.27 × 12/4 = 119 in.	3.20 m

= $b_w + 4h_f$	use 7.25 + 4(2) = 15.25 in.	387 mm
= b	72 in.	1.83 m
Assume neutral axis is in the flange		
$a = f_{pu}mA_p/(0.85f_c'b_{eff})$	425(6)0.11/[(0.85)(6.5)(15.25)] = 3.33 in. > h_f, therefore need to separate forces	84.6 mm
Tendon area for flange		
$A'_p = (b_{eff} - b_w)\,0.85f_c'/f_{pu}$	(15.25 – 7.25) 0.85(6.5)/425 = 0.104 in.²	67.1 mm²
New neutral axis		
$a = (A_p - A'_p)f_{pu}/0.85f_c'b_w)$	(0.66 – 0.104)425/(0.85(6.5)7.25) = 5.90 in.	150 mm
Check tension control		
$\beta_1 = 0.85 - 0.05(f_c' - 4000)/1000$	0.85 – 0.05(6500 – 4000)/1000 = 0.725	0.725
$c/d < 0.375$	= 0(590/0.725)/36 = 0.225 OK	OK
$M_n = A'_p f_{pu}(d - h_f/2) + (A_p - A'_p)f_{pu}(d - a/2)$	0.104(425)(36 – 2/2) + (0.66 – 0.104)425 (36 – 5.9/2) = 9357 in.-kip = 750 ft-kip	1057 kN-m
$\phi M_n > M_u$	0.9(780) = 702 ft-kips > M_u = 481 ft-kips OK	952 kN-m > 544 kN-m
Step 7—Check shear capacity		
Shear capacity will be checked against V_c and, if insufficient, stirrups added		
$\phi V_c = \phi 2\sqrt{f_c'}\,b_wd$	(0.75)2$\sqrt{6500}$ × (7.25 × 36)/1000 = 31.6 kips	140 kN
$\phi V_p = P_ee/L/2$	0.75(90.4)21.45/(32.79 × 12/2) = 7.4 kips	32.9 kN
$\phi V_n = \phi V_c + \phi V_p$	31.6 + 7.4 = 39.0 kips	173 kN
$\phi V_n > V_u$	39.0 kips > 32.7 kips OK	173 kN > 145 kN OK
$V_u > \phi V_c/2$, therefore, minimum shear reinforcement will be required.		
Step 8—Check live load		
Deflections against $L/480$ limit	a_1/L = 16.29/39.37 = 0.413	
$\delta = \dfrac{PL^3(a_1/L)}{24E_cI_g}(3 - 4 \times (a_1/L)^2)$	15(39.37)³0.413(3 – 4 × (0.413)²)1728/(24(4.6 × 10⁶) 51,020) = 0.26 in.	6.6 mm
	δ/L = 0.26/39.37 × 12 = 1/1817 OK	1/1817 OK

Closing comment—The above beam was fabricated as designed by Rocky Mountain Prestress. It was tested to 3,000,000 load cycles producing $6\sqrt{f_c'}$ tensile stress, based on uncracked section. The beam cracked after 100,000 cycles. Following the fatigue test, the beam was loaded to failure. The experimental load capacity was 6% less than the calculated nominal capacity.